

MTOR inhibition attenuates DNA damage and apoptosis through autophagy-mediated suppression of CREB1

Ying Wang, Zhongdong Hu, Zhibo Liu, Rongrong Chen, Haiyong Peng, Jing Guo, Xinxin Chen & Hongbing Zhang

To cite this article: Ying Wang, Zhongdong Hu, Zhibo Liu, Rongrong Chen, Haiyong Peng, Jing Guo, Xinxin Chen & Hongbing Zhang (2013) MTOR inhibition attenuates DNA damage and apoptosis through autophagy-mediated suppression of CREB1, *Autophagy*, 9:12, 2069-2086, DOI: [10.4161/auto.26447](https://doi.org/10.4161/auto.26447)

To link to this article: <https://doi.org/10.4161/auto.26447>



[View supplementary material](#)



Published online: 01 Nov 2013.



[Submit your article to this journal](#)



Article views: 5130



[View related articles](#)



Citing articles: 6 [View citing articles](#)

MTOR inhibition attenuates DNA damage and apoptosis through autophagy-mediated suppression of CREB1

Ying Wang, Zhongdong Hu, Zhibo Liu, Rongrong Chen, Haiyong Peng, Jing Guo, Xinxin Chen, and Hongbing Zhang*

State Key Laboratory of Medical Molecular Biology; Department of Physiology; Institute of Basic Medical Sciences and School of Basic Medicine; Graduate School of Peking Union Medical College; Chinese Academy of Medical Sciences and Peking Union Medical College; Beijing, China

Keywords: apoptosis, autophagy, cAMP response element-binding protein 1, chemoresistance, DNA damage, mechanistic target of rapamycin

Abbreviations: ATG5, autophagy-related 5; ATG7, autophagy-related 7; CREB1, cAMP responsive element binding protein 1; DAPI, 4', 6'-diamidino-2-phenylindole; DMSO, dimethyl sulfoxide; DSBs, double-strand breaks; FACS, fluorescence-activated cell sorting; FITC, fluorescein isothiocyanate; LC3, microtubule-associated protein 1 light chain 3; 3-MA, 3-methyladenine; MEFs, mouse embryonic fibroblasts; MTOR, mechanistic target of rapamycin; MTT, 3-[4, 5-dimethyl-thiazol-2yl] 2, 5-diphenyltetrazoliumbromide; PARP1, poly (ADP-ribose) polymerase 1; PCR, polymerase chain reaction; PBS, phosphate-buffered saline; PI, propidium iodide; PTEN, phosphatase and tensin homolog; siRNA, small interfering RNA; SQSTM1, sequestosome 1; TSC, tuberous sclerosis complex; WT, wild type

Hyperactivation of mechanistic target of rapamycin (MTOR) is a common feature of human cancers, and MTOR inhibitors, such as rapamycin, are thus becoming therapeutics in targeting certain cancers. However, rapamycin has also been found to compromise the efficacy of chemotherapeutics to cells with hyperactive MTOR. Here, we show that loss of TSC2 or PTEN enhanced etoposide-induced DNA damage and apoptosis, which was blunted by suppression of MTOR with either rapamycin or RNA interference. cAMP response element-binding protein 1 (CREB1), a nuclear transcription factor that regulates genes involved in survival and death, was positively regulated by MTOR in mouse embryonic fibroblasts (MEFs) and cancer cell lines. Silencing *Creb1* expression with siRNA protected MTOR-hyperactive cells from DNA damage-induced apoptosis. Furthermore, loss of TSC2 or PTEN impaired either etoposide or nutrient starvation-induced autophagy, which in turn, leads to CREB1 hyperactivation. We further elucidated an inverse correlation between autophagy activity and CREB1 activity in the kidney tumor tissue obtained from a TSC patient and the mouse livers with hepatocyte-specific knockout of PTEN. CREB1 induced DNA damage and subsequent apoptosis in response to etoposide in autophagy-defective cells. Reactivation of CREB1 or inhibition of autophagy not only improved the efficacy of rapamycin but also alleviated MTOR inhibition-mediated chemoresistance. Therefore, autophagy suppression of CREB1 may underlie the MTOR inhibition-mediated chemoresistance. We suggest that inhibition of MTOR in combination with CREB1 activation may be used in the treatment of cancer caused by an abnormal PI3K-PTEN-AKT-TSC1/2-MTOR signaling pathway. CREB1 activators should potentiate the efficacy of chemotherapeutics in treatment of these cancers.

Introduction

Inappropriate cellular responses to stress changes within and outside the cells may facilitate the development of many tumors. The MTOR (mechanistic target of rapamycin) serves as a major effector that regulates diverse key cellular processes, such as cell growth,¹ differentiation,² metabolism,³ and autophagy.⁴ Dysregulation of MTOR signaling caused by loss-of-function mutations of tumor suppressors including PTEN (phosphatase and tensin homolog),⁵ TSC (tuberous sclerosis complex)^{1/2,}^{6–11}

or STK11/LKB1 (serine/threonine kinase 11),¹² and gain-of-function mutations of proto-oncogenes such as PI3K (phosphoinositide 3-kinase)¹³ or AKT (v-akt murine thymoma viral oncogene homolog 1)^{7,13} is a frequent event in human cancers.¹⁴ Thus, MTOR is presented as an attractive target for cancer therapy. Rapamycin, a highly specific inhibitor of MTOR, has been shown as a therapeutic reagent for cancers driven by aberrant activation of MTOR signaling.¹⁵ However, rapamycin also promotes the survival of chemotherapeutics treated cells through some underlying mechanisms such as AMPK-dependent

*Correspondence to: Hongbing Zhang; Email: hbzhang@ibms.pumc.edu.cn or hbzhang2006@gmail.com
Submitted: 01/12/2013; Revised: 09/03/2013; Accepted: 09/10/2013
<http://dx.doi.org/10.4161/auto.26447>

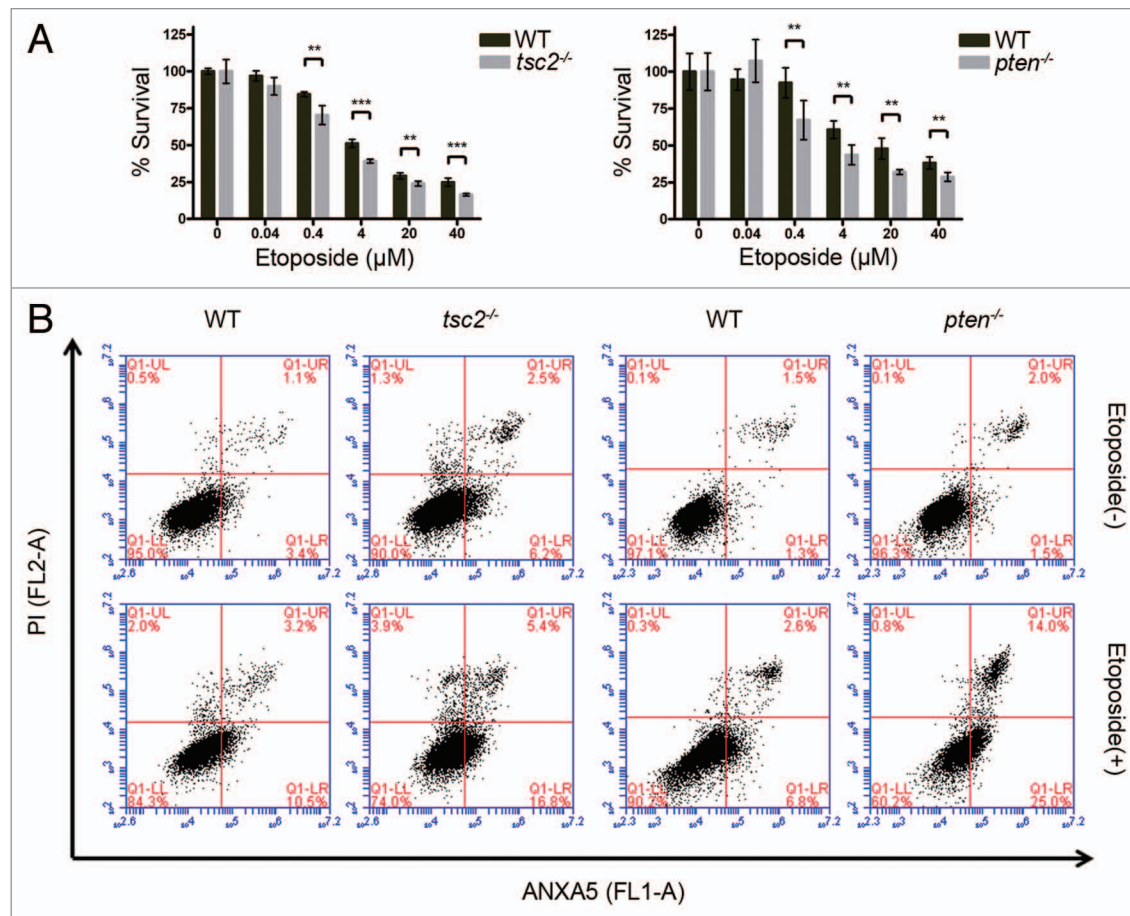


Figure 1A and B. Hyperactive MTOR sensitizes TSC2- or PTEN-deficient cells to etoposide-mediated DNA damage and apoptosis. **(A)** Reduced viability of *tsc2^{-/-}* or *pten^{-/-}* MEFs treated with etoposide. *tsc2^{-/-}* or *pten^{-/-}* MEFs and their WT counterparts were treated with etoposide for 48 h at the indicated concentration. Cell viability was determined with the MTT assay. ***P* < 0.01, ****P* < 0.001. **(B)** Loss of TSC2 or PTEN increased etoposide-induced apoptosis as illustrated by an increase of total ANXA5-positive cells (LR+UR quadrants). After etoposide treatment for 24 h, apoptosis induction was analyzed by FACS. Cells in the LR (lower right) and UR (upper right) quadrants were considered early apoptotic (ANXA5-FITC positive, PI negative), late apoptotic, and necrotic (ANXA5-FITC positive, PI positive), respectively.

inactivation of TP53/p53¹⁶ and increased activation of survival kinases.¹⁷⁻¹⁹

CREB1 (cAMP responsive element binding protein 1) is a nuclear transcription factor which regulates target genes involved in cell survival and cell death. Upon the activation of cAMP-dependent signal transduction, CREB1 is activated via phosphorylation at Ser133 by PRKA.^{20,21} Overexpression and hyperactivation of CREB1 are often observed in acute myeloid leukemia^{22,23} and several human solid malignancies such as breast,²⁴ lung,²⁵ ovary,²⁶ and prostate²⁷ carcinomas. Inhibition of CREB1 in several human cancer cell lines causes induction of apoptosis and suppression of cell proliferation,^{22,28} indicative of its critical role as a proto-oncogene. Conversely, several studies have demonstrated that stimulation of cAMP pathway inhibits proliferation of some human cancer cell lines²⁸ and induces apoptosis of Ras-mutated melanoma cell lines.²⁹ In addition, CREB1 activation, due to dysfunction in mitochondria, impairs cell proliferation.³⁰ Therefore, the precise role of CREB1 in cancer development is still uncertain. Furthermore, neither its role in cancer therapy nor the mechanism governing its activity and expression in cancer is fully understood.

Autophagy is a self-cannibalization process that begins with sequestering cell structures in double-membrane vesicles (autophagosomes), and then targets them for degradation by fusion of autophagosomes and lysosomes (autolysosomes).³¹ This “self-eating” process exerts important roles in many aspects of physiology and pathology, including intracellular homeostasis, cell death, tumor suppression, and aging.^{32,33} Recently, it has been reported that induction of autophagy is frequently observed in many human cancer cell lines treated with chemotherapeutics.³⁴⁻³⁶ However, whether autophagy induced by chemotherapy acts as a protective mechanism that allows treated cancer cells to survive or rather as an alternative cell death-inducing process has been an issue of great controversy. Although MTOR plays an inhibitory role in regulation of autophagy, little is known about the role of autophagy in the chemotherapy of cancers driven by aberrant activation of MTOR signaling.

In this study, we sought to explore the mechanism by which MTOR inhibition results in chemoresistance. We identified CREB1 as a new target involved in MTOR-modulated autophagy signaling cascade and found that autophagy impairment

Figure 1C and D. Hyperactive MTOR sensitizes TSC2- or PTEN-deficient cells to etoposide-mediated DNA damage and apoptosis. (C) Loss of TSC2 or PTEN led to increased accumulation of γ-H2A.X protein and PARP1 cleavage after 24 h etoposide treatment. (D) *tsc2*^{-/-} or *pten*^{-/-} MEFs accumulated more γ-H2A.X foci post-etoposide treatment. Cells were fixed and stained with anti-γ-H2A.X antibody and the etoposide-induced foci (green) were visualized with immunofluorescence. DNA was counterstained with DAPI (blue). Representative images are shown. The γ-H2A.X foci were quantified by counting at least 200 cells and the numbers of the foci between WT and *tsc2*^{-/-} or *pten*^{-/-} MEFs treated with etoposide were then compared.

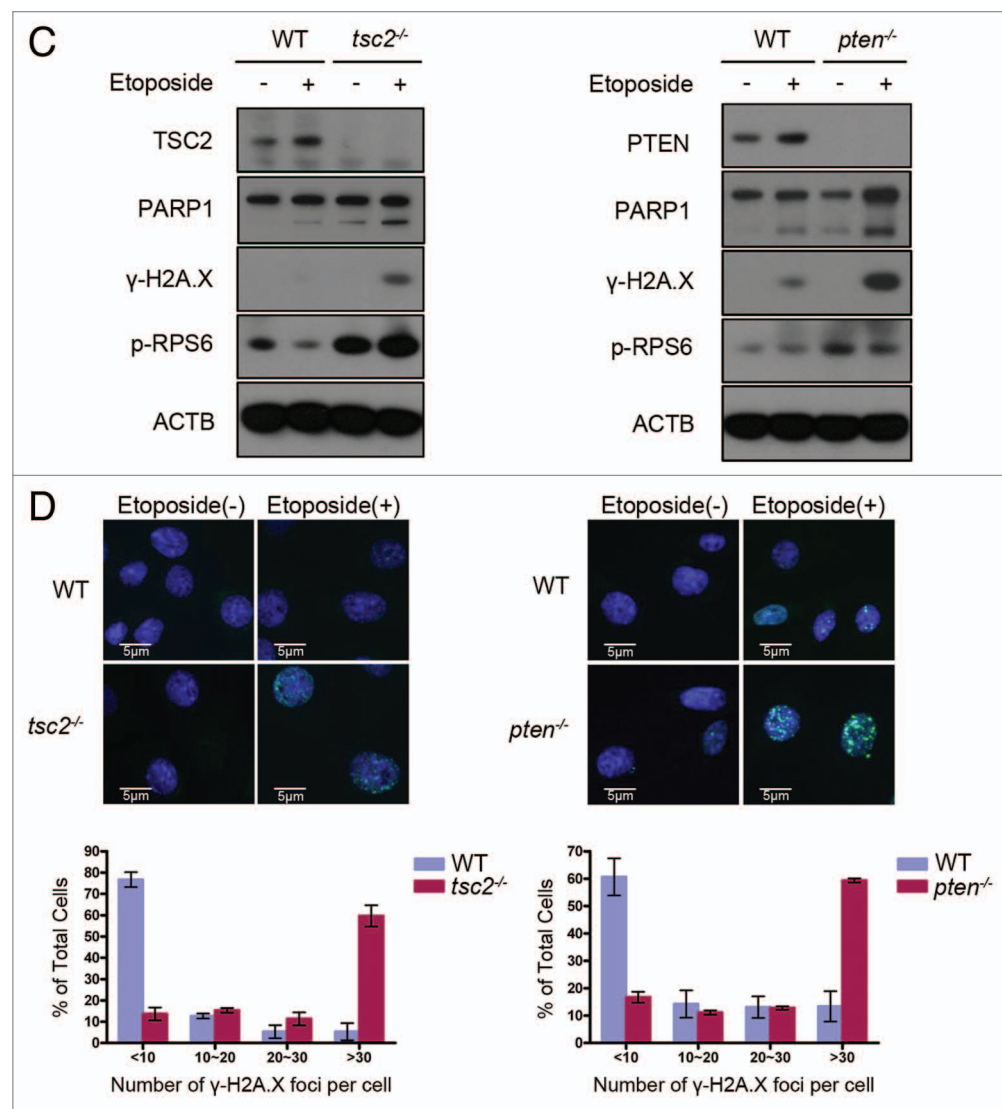
due to constitutive MTOR activation is sufficient to trigger CREB1 phosphorylation and accumulation. Under conditions of etoposide-induced genomic damage, CREB1 activation induced by impaired autophagy had a growth disadvantage and an enhanced DNA damage in MTOR-hyperactivated cells. Therefore, MTOR inhibition-mediated chemoresistance is a result of CREB1 suppression via induction of autophagy. Our findings may have therapeutic implication for the treatment of cancers driven by aberrant activation of MTOR signaling.

Results

Inhibition of MTOR induces resistance to etoposide

The PTEN and TSC1/2 tumor suppressor proteins tightly control MTOR activity. Loss of these tumor suppressors leads to constitutive MTOR activation. To investigate MTOR inhibition-mediated effect on cell survival in response to chemotherapy, we treated *tsc2*^{-/-} and *pten*^{-/-} mouse embryonic fibroblasts (MEFs) with 0.04 to 40 μM of etoposide for 48 h. Compared with that of wild-type (WT) MEFs, the viability of *tsc2*^{-/-} and *pten*^{-/-} MEFs were significantly decreased by etoposide in a dose-dependent manner (Fig. 1A). Similarly, cells deficient in TSC2 or PTEN are more sensitive to cisplatin treatment than WT cells (Fig. S1).

DNA-damaging agents can induce cell death via either apoptosis or necrosis. To determine whether hyperactive MTOR-enhanced etoposide-induced global cell death is apoptotic or necrotic, we analyzed cell death by using ANXA5/annexin



A5-FITC/propidium iodide (PI) staining followed by flow cytometry. Since the dying cells induced by etoposide were mainly stained by ANXA5 and not PI, the cell death was thus predominately apoptotic (Fig. 1B). Consistent with their etoposide-sensitive phenotype (Fig. 1A), MTOR-hyperactivated cells showed higher apoptotic rate in response to etoposide, comparing to their control WT cells. To determine the extent of induction of apoptosis and confirm the FACS analysis results, we further analyzed a biochemical hallmark of apoptosis—PARP1 [poly (ADP-ribose) polymerase 1] cleavage. PARP1 is an abundant nuclear protein and its roles in various DNA metabolic activities are well established. It is cleaved in apoptotic cells by CASP3 (caspase 3)³⁷ in response to many DNA-damaging agents including etoposide. Consistent with the FACS data, higher level of cleaved PARP1 was observed in MTOR-hyperactivated cells, compared with that in WT cells (Fig. 1C).

Since etoposide is an inducer of double-strand breaks (DSBs) in DNA, we proposed that constitutive MTOR activation could facilitate cell death induced by chemotherapy through persistent DNA damage response. Detection and visualization of H2AFX

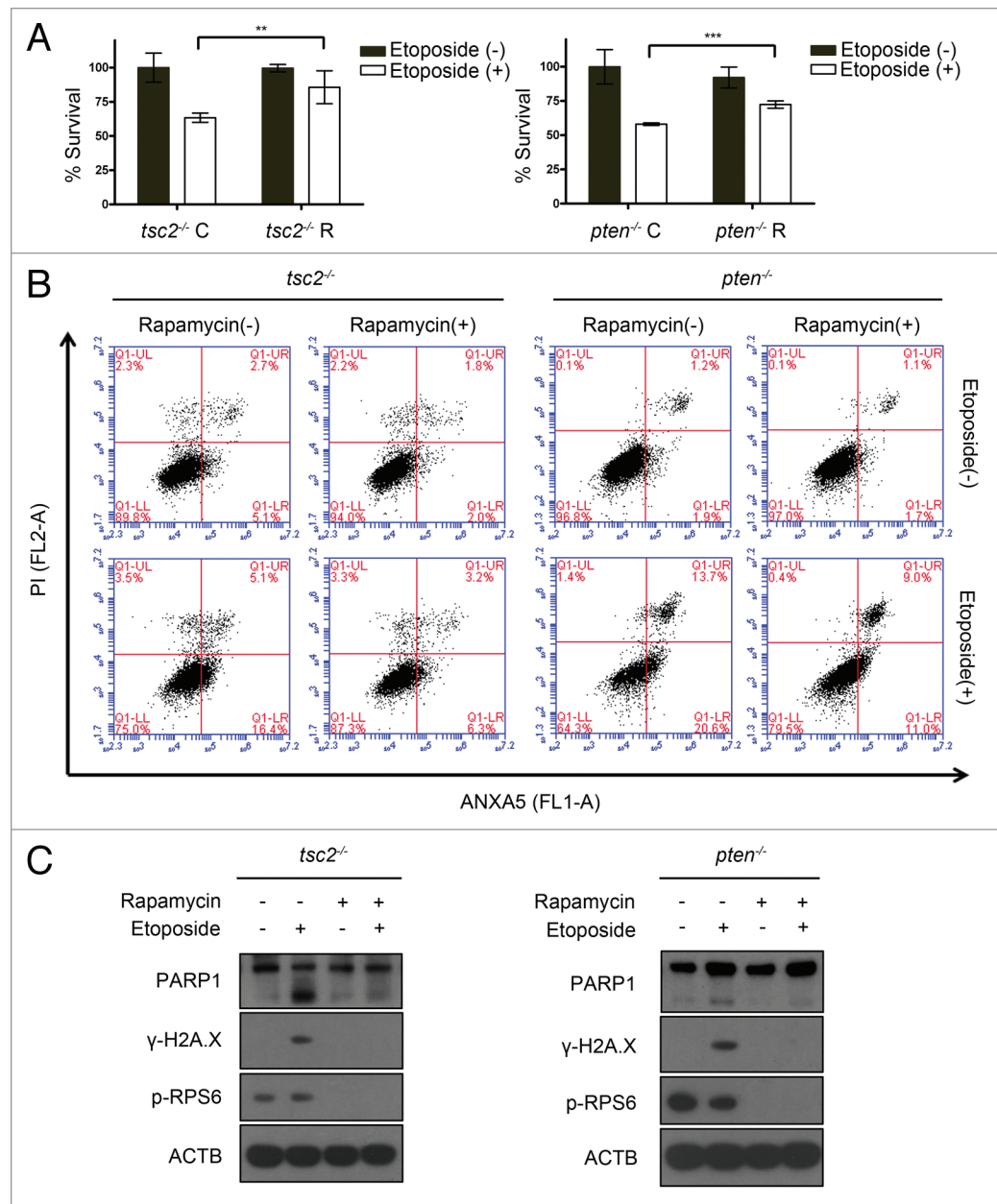


Figure 2A–C. Suppression of MTOR protects cells from DNA damage-induced apoptosis. *tsc2*^{-/-} or *pten*^{-/-} MEFs were pretreated with or without 10 nM rapamycin for 6 h (A–C), or were transfected with nontargeting control siRNA or *Mtor*-specific siRNA (D–F) before they were exposed to etoposide. MTOR suppression by rapamycin (A) or specific siRNA (D) increased the viability of cells after etoposide treatment. Cell viability was analyzed with the MTT assay. ***P* < 0.01, ****P* < 0.001. FACS analysis showed that either rapamycin pretreatment (B) or MTOR knockdown (E) protected against etoposide-induced apoptosis. Cells gated in LR and UR quadrants were considered apoptotic. Immunoblotting analysis revealed that rapamycin (C) or MTOR knockdown (F) suppressed the induction of γ -H2A.X protein and PARP1 cleavage in *tsc2*^{-/-} or *pten*^{-/-} MEFs 24 h post-etoposide treatment.

phosphorylated on Ser139 (γ -H2A.X) by western blotting and immunofluorescence were performed to assess DNA DSBs³⁸ after chemotherapy in MTOR-hyperactivated cells. As shown in Figure 1C, treatment of all types of cells with etoposide led to an increase of γ -H2A.X protein 24 h post-therapeutic reagent administration. However, the level of γ -H2A.X expression was much higher in *tsc2*^{-/-} or *pten*^{-/-} MEFs than in WT MEFs. In addition, both of WT MEFs and MTOR-hyperactivated MEFs showed very few γ -H2A.X foci without etoposide treatment, while the foci increased significantly in all types of cells in the presence of etoposide. However, more than 60% WT MEFs had < 10 foci per cell, whereas approximately 60% MTOR-hyperactivated MEFs had > 30 foci per cell (Fig. 1D).

Moreover, preinhibition of MTOR by rapamycin increased the cell viability (Fig. 2A) and decreased the apoptotic rate (Fig. 2B) of *tsc2*^{-/-} or *pten*^{-/-} MEFs treated with etoposide. As expected,

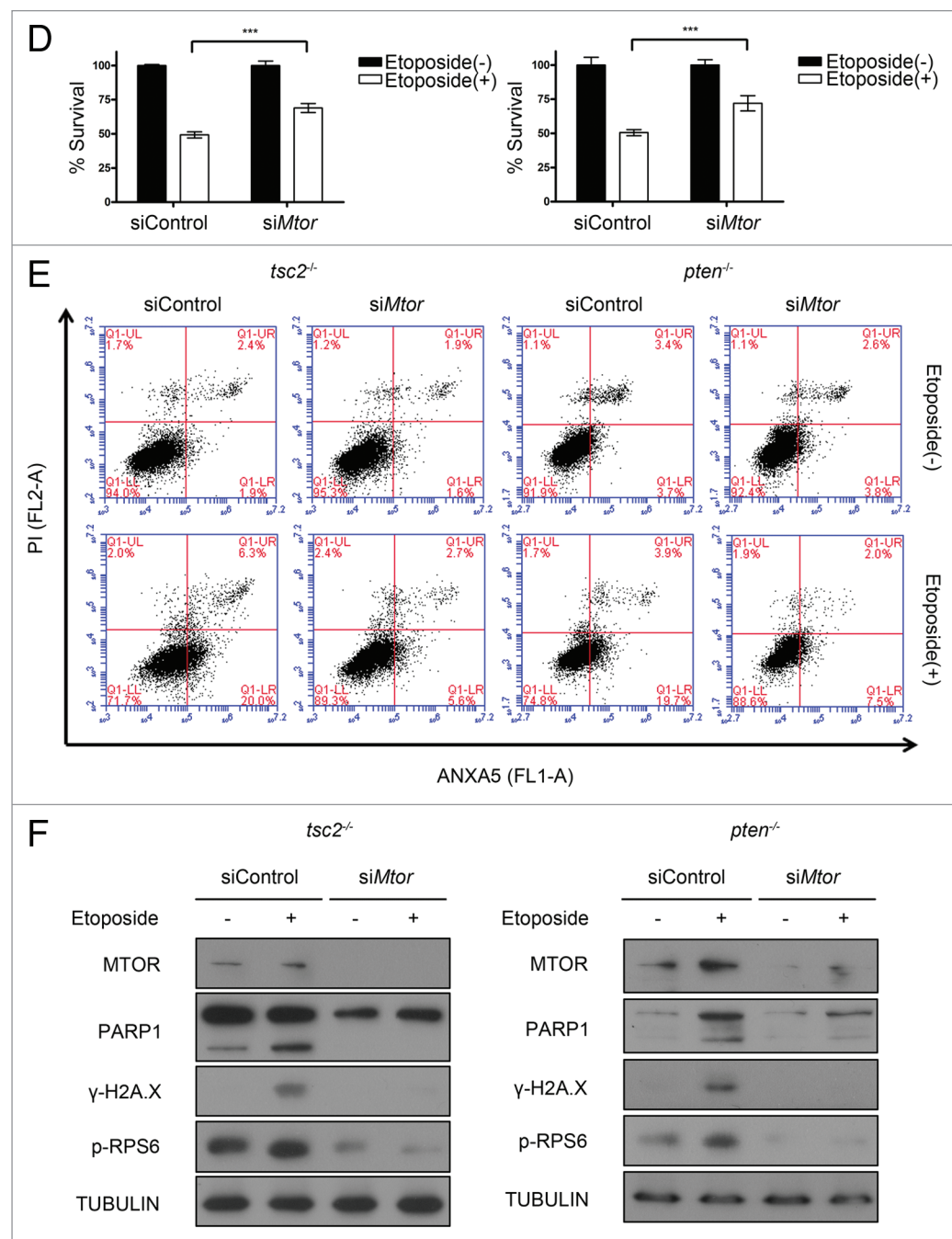
the level of γ -H2A.X expression and cleaved PARP1 were greatly reduced in *tsc2*^{-/-} or *pten*^{-/-} MEFs treated with etoposide when MTOR was preinhibited by rapamycin (Fig. 2C). To confirm the cell responses caused by inhibition of MTOR, specific siRNA targeted against *Mtor* was used to reduce MTOR in *tsc2*^{-/-} or *pten*^{-/-} MEFs. Consistent with rapamycin's effect on *tsc2*^{-/-} or *pten*^{-/-} MEFs, MTOR knockdown protected these cells from etoposide-induced apoptotic cell death, as evidenced by elevation of cell viability (Fig. 2D) and reduction of apoptotic rate (Fig. 2E), γ -H2A.X expression and cleaved PARP1 (Fig. 2F). Taken together, these results indicated that constitutive MTOR activation sensitizes cells to DNA damage-induced apoptotic cell death, while inhibition of MTOR reduces etoposide-induced DNA damage and therefore induces resistance to etoposide.

MTOR enhances etoposide-induced CREB1 activation

An inverse correlation has been found between STK11 protein levels and CREB1 activity,^{39,40} suggesting a role of STK11 in the activation of CREB1 signaling. In addition, loss of STK11 can lead to constitutive activation of MTOR.¹² We speculated that there might be a link between MTOR and CREB1 signaling. To explore whether CREB1 was involved in MTOR regulation of DNA damage, we determined the activity of CREB1

Figure 2D–F. *tsc2*^{-/-} or *pten*^{-/-} MEFs were transfected with nontargeting control siRNA or MTOR-specific siRNA (D–F) before they were exposed to etoposide. MTOR suppression by specific siRNA (D) increased the viability of cells after etoposide treatment. For more information, see the Figure 2A–C legend.

in response to chemotherapy by examining its phosphorylation and accumulation in WT MEFs and MTOR-hyperactivated MEFs. As represented in Figure 3A, in response to etoposide treatment, phosphorylation of CREB1 on Ser133 and accumulation of total CREB1 protein were markedly induced in *tsc2*^{-/-} MEFs. Moreover, the phosphorylation and accumulation of CREB1 were reduced by rapamycin with or without etoposide treatment (Fig. 3B). Similar findings were also obtained from *pten*^{-/-} MEFs (Fig. 3C and D). In addition, cisplatin treatment also resulted in a dramatic activation of CREB1 in the MEFs with MTOR hyperactivation due to deletion of either *Tsc2* or *Pten*, in comparison with WT MEFs (Fig. S2). Other than MEFs, we evaluated the regulation of MTOR on CREB1 activation in 3 cancer cell lines as well as a TSC2-deficient ELT-3 cell line derived from a uterine leiomyoma in an Eker rat with a germline insertion in the *Tsc2* gene.^{41,42} As shown in Figure 3E, rapamycin reduced the phosphorylation and accumulation of CREB1 in all cell lines. The inhibitory effect of rapamycin on the phosphorylation and accumulation of CREB1 indicates that the different state of MTOR activation was responsible for the differential response of CREB1 to chemotherapy between WT MEFs and *tsc2*^{-/-} or *pten*^{-/-} MEFs. Furthermore, we found that knockdown of MTOR in *tsc2*^{-/-} or *pten*^{-/-} cells significantly reduced the phosphorylation and accumulation of CREB1 protein with or without etoposide treatment (Fig. 3F). The reduced CREB1 activation caused by MTOR knockdown further supports our finding that MTOR positively regulates CREB1 activity.



To ensure that phosphorylated CREB1 is capable of regulating gene expression, we examined the expression of c-FOS (FOS), a CREB1-regulated immediate-early gene.⁴³ As can be seen in Figure 4A, etoposide-induced *Fos* mRNA expression was reversed by rapamycin in *tsc2*^{-/-} MEFs. Consistently, in response to etoposide, the protein level of FOS was also greatly increased, and was markedly reduced by rapamycin treatment in *tsc2*^{-/-} MEFs (Fig. 4B). Furthermore, the overexpression of M1-CREB1, a dominant-negative mutant for CREB1,⁴⁴ significantly inhibited the phosphorylation of endogenous CREB1 and the protein level of FOS (Fig. 4C). Taken together, these data suggest that MTOR is a positive regulator of CREB1 activity and CREB1 may play a role in MTOR regulation of etoposide-induced DNA damage response.

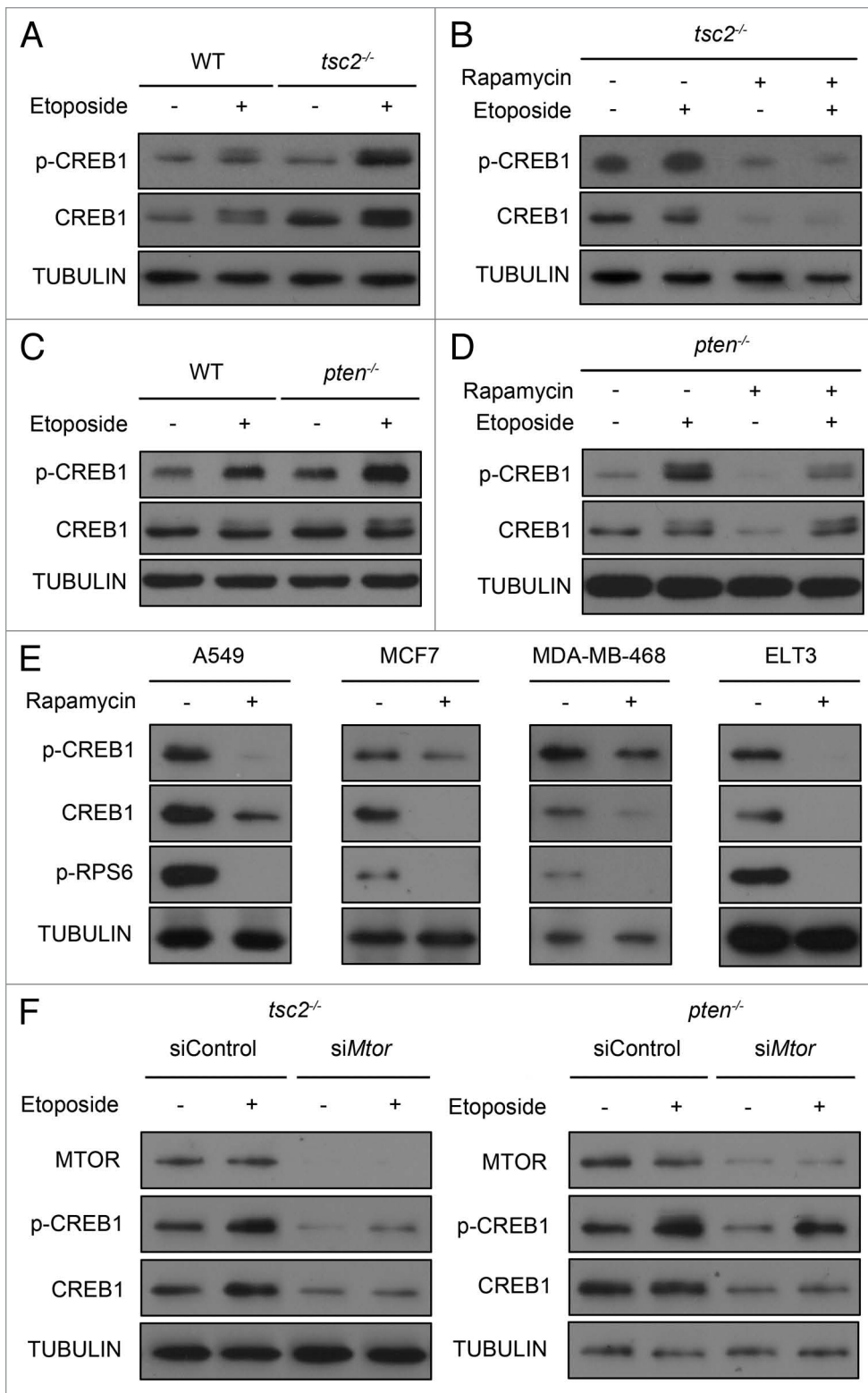


Figure 3. CREB1 activation in response to etoposide depended on MTOR. Total protein lysates were harvested from cells for immunoblotting (**A–F**). Loss of TSC2 (**A**) or PTEN (**C**) led to enhanced phosphorylation and accumulation of CREB1 protein after 24 h of etoposide treatment. Rapamycin pretreatment reduced the phosphorylation and accumulation of CREB1 protein in *tsc2*^{-/-} (**B**) or *pten*^{-/-} MEFs (**D**) with or without etoposide treatment for 24 h. (**E**) MTOR positively regulated the phosphorylation and accumulation of CREB1 in cancer cell lines. Cells were treated with or without 10 nM rapamycin for 6 h. (**F**) MTOR knockdown suppressed the phosphorylation and accumulation of CREB1 in *tsc2*^{-/-} or *pten*^{-/-} MEFs with or without etoposide treatment.

MTOR promotes etoposide-induced DNA damage response through activation of CREB1

cAMP, which can trigger the activation of CREB1, has been reported to sensitize cells to pro-apoptotic agents.²⁹ Moreover, CREB1 has been implicated in the enhanced expression of CCND1 (cyclin D1),⁴⁵ BID,⁴⁶ TP53, and CDKN1A/p21.^{30,47} Since cAMP, CCND1, BID, TP53, and CDKN1A are involved in the DNA damage response,^{46,48–51} we proposed that the enhanced phosphorylation and accumulation of CREB1 might be necessary to mediate the effect of constitutive MTOR activation on DNA damage and subsequent apoptosis in response to etoposide. By silencing *Creb1* gene expression with RNA interference in MTOR-hyperactivated MEFs, we found that suppression of CREB1 inhibited hyperactive MTOR-enhanced DNA damage as evidenced by decreased γ -H2A.X expression (Fig. 5A) and promoted cell survival in the presence of etoposide (Fig. 5B). We next demonstrated that suppression of CREB1 attenuated DNA damage-induced apoptosis of MTOR-hyperactivated cells, as manifested by fewer ANXA5-positive cells (Fig. 5C) and decreased PARP1 cleavage (Fig. 5D) in CREB1 knockdown cells than in control cells.

To exclude the possibility that CREB1 is functionally distinct in promotion of DNA damage-induced apoptosis of MEFs in our study, we examined CREB1's effect on DNA damage-induced apoptosis in TSC2-deficient ELT-3 cells. When CREB1 was knocked down in ELT-3 cells, γ -H2A.X induction and PARP1 cleavage were inhibited (Fig. 5D) and ANXA5-positive cells were decreased (Fig. 5E). In addition, we used a specific activator of CREB1 to confirm that activation of CREB1 was able to trigger apoptosis induced by etoposide. When CREB1 was stimulated in WT MEFs with forskolin,

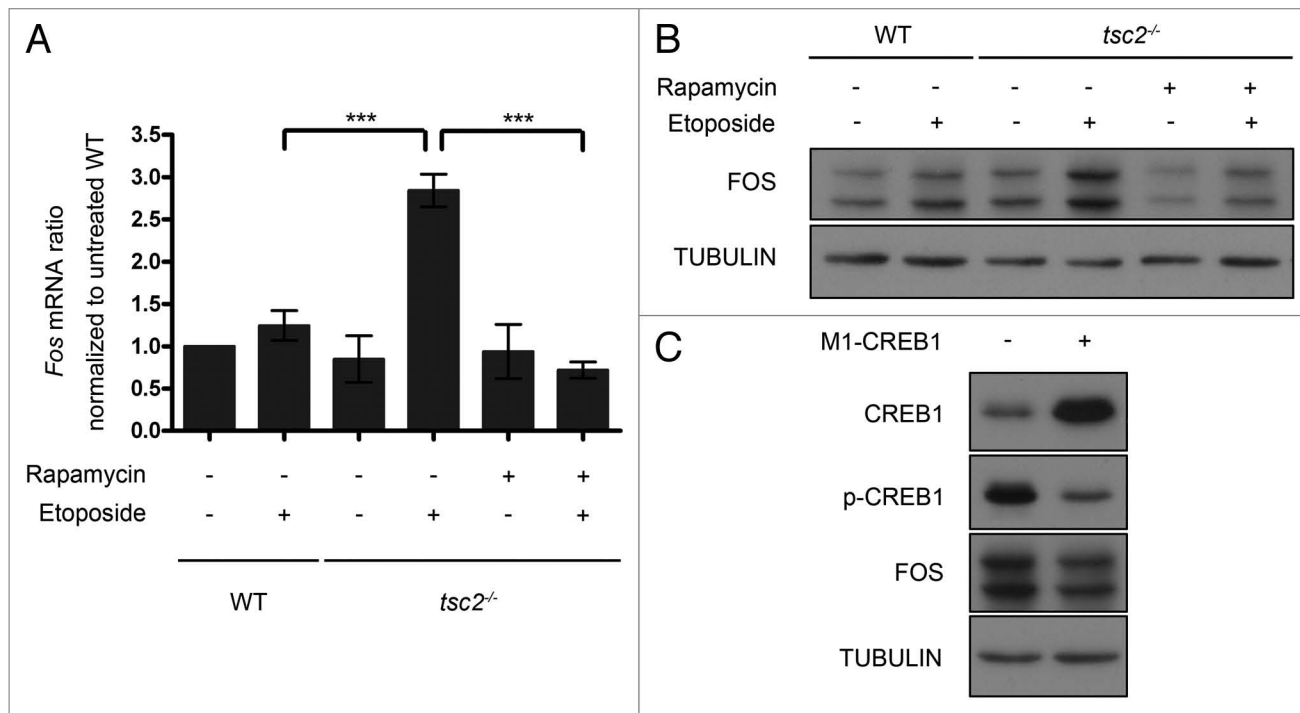


Figure 4. MTOR positively regulates etoposide-induced FOS expression. **(A)** MTOR positively regulated etoposide-induced *Fos* mRNA expression. Quantitative real-time PCR analysis of *Fos* mRNA in WT cells, *tsc2*^{-/-} MEFs and rapamycin-pretreated *tsc2*^{-/-} MEFs with or without addition of etoposide for 24 h. **(B)** Immunoblotting of FOS expression in WT cells, *tsc2*^{-/-} MEFs and rapamycin-pretreated *tsc2*^{-/-} MEFs with or without addition of etoposide for 24 h. **(C)** Effect of dominant-negative mutant M1-CREB1 overexpression on phosphorylation of the endogenous CREB1 and FOS expression in *tsc2*^{-/-} MEFs. Cells overexpressed with or without M1-CREB1 were subjected to immunoblotting.

a cAMP agonist, DNA damage-induced apoptotic cell death was enhanced, as evidenced by reduced cell viability, and elevated γ -H2AX induction, PARP1 cleavage and apoptotic rate (Fig. 5F–H). Taken together, these data demonstrate that hyperactive MTOR promotes etoposide-induced DNA damage via increased CREB1 activity.

MTOR activates etoposide-induced CREB1 through suppression of autophagy

Since autophagy signaling is downstream of MTOR, CREB1 might be modulated by MTOR through suppression of autophagy. To explore the role of autophagy in the regulation of CREB1 activity, we first examined the effect of etoposide on the induction of autophagy in *tsc2*^{-/-}, *pten*^{-/-}, and WT MEFs. Redistribution of the autophagy protein LC3 from a diffused staining pattern throughout the cytoplasm and nucleus to cytoplasmic puncta is a hallmark of autophagy induction (formation of autophagosomes).⁵² As evident from Figure 6A, all types of MEFs showed diffused distribution of LC3 in the absence of etoposide under a fluorescence microscope. However, treatment of etoposide increased LC3 puncta in number and intensity in WT MEFs rather than in *tsc2*^{-/-} or *pten*^{-/-} MEFs. For quantification of the induction of autophagic cells, at least 200 cells of each type were counted for every treatment. As shown in Figure 6B, more than 80% of WT MEFs treated with etoposide showed LC3 puncta, while these autophagic features were observed in less than 20% of MTOR-hyperactivated MEFs. Since the accumulation of autophagosomes may represent either the increased

generation of autophagosomes or a blockade in autophagosome maturation, autophagosome formation does not always indicate increased autophagic activity.⁵² Hence, expression of sequestosome 1/p62 (SQSTM1) that inversely correlates with autophagic activity was also examined. Consistent with increased autophagosomes in WT MEFs after the treatment with etoposide, SQSTM1 was markedly decreased in WT MEFs. In contrast, SQSTM1 degradation was not observed in *tsc2*^{-/-} or *pten*^{-/-} MEFs treated with etoposide, indicating that autophagy in these cells is defective (Fig. 6C). In addition, the autophagic flux observed in WT MEFs was also measured by inferring LC3-II turnover in the presence or absence of lysosomal degradation.⁵³ By using immunoblotting analysis, we found that etoposide induced LC3-II in WT cells but not TSC2-deficient cells (Fig. S3). This was further verified by inhibition of the “autophagic flux” with baflomycin A₁, which prevents maturation of autophagic vacuoles by inhibiting fusion of autophagosomes and lysosomes,⁵⁴ resulting in a further accumulation of LC3-II in WT cells (Fig. S3). Furthermore, pretreatment of rapamycin markedly restored autophagy as shown by the degradation of SQSTM1 in *tsc2*^{-/-} or *pten*^{-/-} MEFs treated with or without etoposide (Fig. 6D).

To investigate whether the difference in CREB1 response between WT MEFs and MTOR-hyperactivated MEFs was due to the distinction in autophagy stimulation upon etoposide treatment, we examined the effect of pharmacological and genetic manipulations of autophagy on CREB1 in response to etoposide. As shown in Figure 7A, treatment of WT MEFs

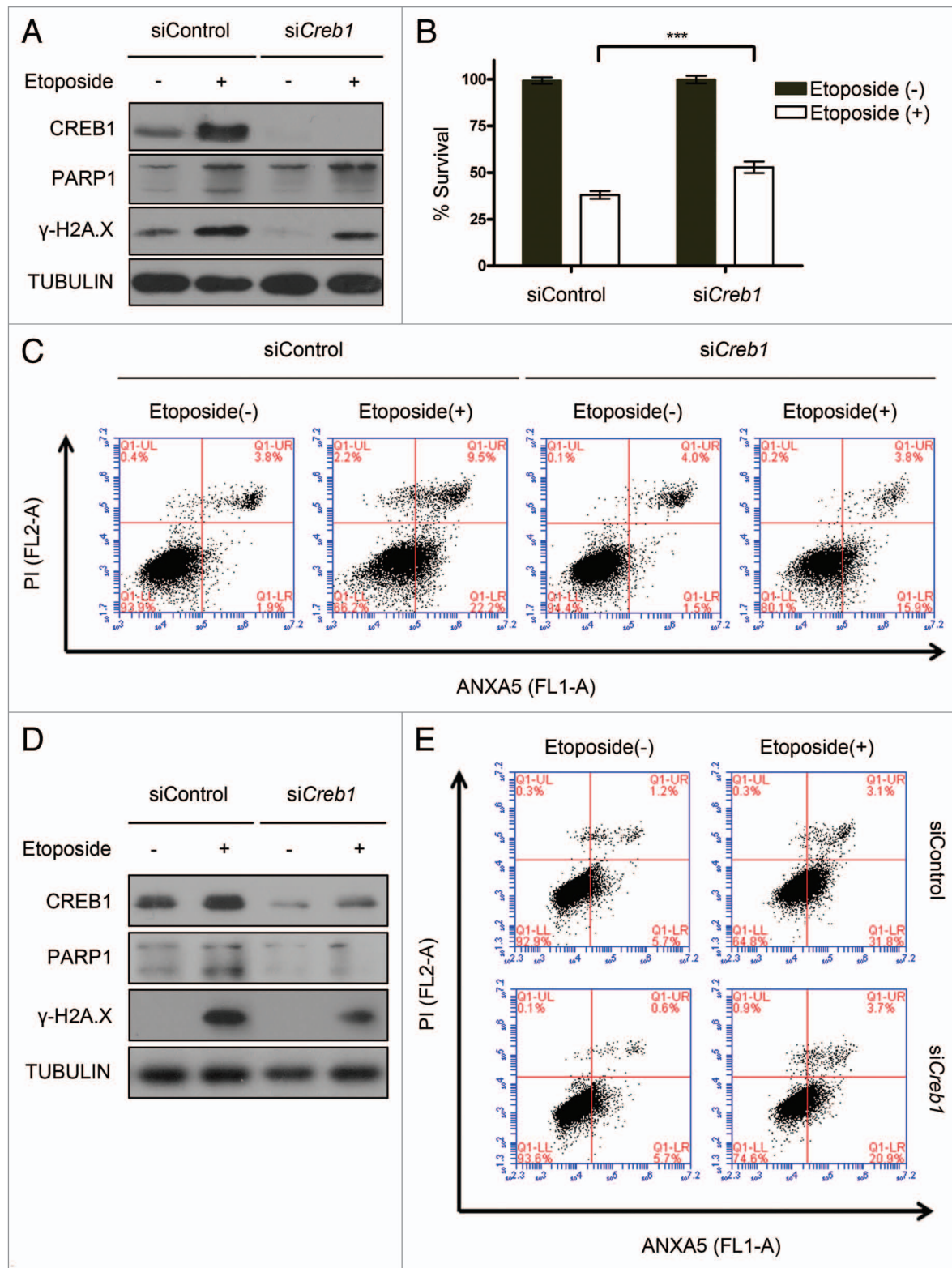


Figure 5A–E. CREB1 is required for MTOR-mediated enhancement of DNA damage and apoptosis. *tsc2^{-/-}* MEFs (**A–C**) or ELT3 cells (**D–E**) transfected with nontargeting control siRNA or *Crb1* specific siRNA were subsequently exposed to etoposide. (**A**) Reduction of CREB1 decreased the induction of γ -H2A.X protein and PARP1 cleavage in etoposide-treated *tsc2^{-/-}* MEFs. (**B**) Reduction in CREB1 increased the viability of etoposide-treated *tsc2^{-/-}* MEFs. Cell viability was determined with the MTT assay. ***P < 0.001. (**C**) FACS analysis showed that CREB1 knockdown protects cells against etoposide-induced apoptosis. The percentage of cells gated in LR and UR quadrants represents the extent of apoptosis. (**D**) CREB1 knockdown suppressed the induction of γ -H2A.X protein and PARP1 cleavage of ELT3 cells in response to etoposide. (**E**) The percentage of apoptotic cells gated in LR and UR quadrants was decreased after treatment with siRNA against CREB1 in etoposide-treated ELT3 cells.

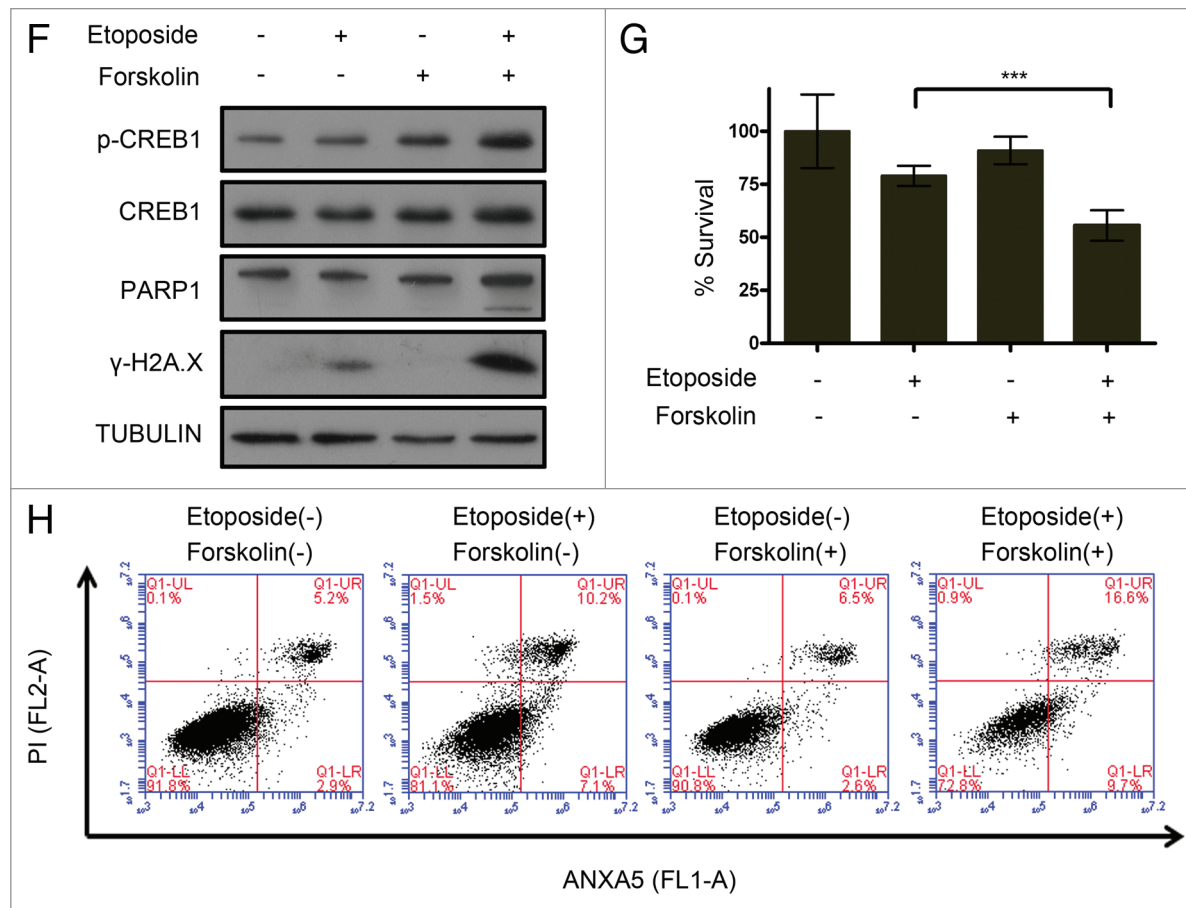


Figure 5F–H. CREB1 is required for MTOR-mediated enhancement of DNA damage and apoptosis. WT MEFs were treated with either etoposide, or forskolin, or etoposide in combination with forskolin (F–H). (F) cAMP stimulation by forskolin enhanced the phosphorylation of CREB1 and promotes the induction of γ -H2A.X and PARP1 cleavage. (G) cAMP stimulation by forskolin inhibited the viability of cells treated with etoposide. Cell viability was determined with the MTT assay. *** $P < 0.001$. (H) Apoptosis was increased after cells were treated with forskolin as depicted by an increase of total ANXA5-positive cells (LR+UR quadrants).

with 3-methyladenine (3-MA), a specific inhibitor of autophagy that inhibits autophagy at an early stage by blocking autophagic sequestration, resulted in an enhanced response of CREB1 to etoposide treatment. This inhibitory effect of autophagy on CREB1 activity upon etoposide treatment was further confirmed in MEFs genetically deficient in autophagy-related genes, as indicated by a marked increase in the phosphorylation and accumulation of CREB1 in *atg5*^{−/−} or *atg7*^{−/−} MEFs treated with or without etoposide (Fig. 7B). Furthermore, ATG5 knockdown significantly elevated the phosphorylation and accumulation of CREB1 in the human lung cancer cell line A549 with or without etoposide treatment (Fig. 7C).

To further validate the negative role of autophagy in CREB1 activity, we examined the effect of a potent autophagy stimulus, nutrient deprivation medium, on CREB1 activity. In agreement with a recent finding,⁵⁵ the percentage of autophagic cells among WT MEFs was markedly increased after 4 h nutrient starvation but steadily decreased to a very low level after 12 h nutrient starvation (Fig. S4). These dynamic changes inversely correlated with the expression of SQSTM1 during starvation (Fig. 7D). An impaired induction of autophagy was observed in MTOR-hyperactivated

MEFs during nutrient starvation, as there was a slight decrease in SQSTM1 protein level (Fig. 7D) and very few autophagic cells among *tsc2*^{−/−} MEFs during starvation (Fig. S4). Accordingly, we observed dynamic fluctuation of CREB1 activity which inversely correlates with state of starvation-induced autophagy in both WT MEFs and MTOR-hyperactivated MEFs, as both SQSTM1 and CREB1 were reduced after 4 h nutrient starvation, but restored by 8 h and thereafter (Fig. 7D; Fig. S5). Nevertheless, CREB1 activity in MTOR-hyperactivated MEFs was higher than that in WT MEFs at each time point of starvation (Fig. 7D; Fig. S5). Furthermore, inhibition of autophagy in WT MEFs with either 3-MA or knockout of autophagy-related genes reversed the inhibitory effect of nutrient starvation on CREB1 phosphorylation (Fig. 7E; Fig. S6), suggesting that autophagy negatively regulates CREB1 activity. To explore whether this newly identified mechanism of MTOR regulation of CREB1 through suppression of autophagy exists in vivo, we examined tissues obtained from kidney angiomyolipoma driven by hyperactive MTOR due to *TSC2* mutation from a TSC patient. SQSTM1 and phosphorylation of CREB1 on Ser133 were higher in the kidney tumor tissue than in paraneoplastic kidney tissue (Fig. 7F). We also examined

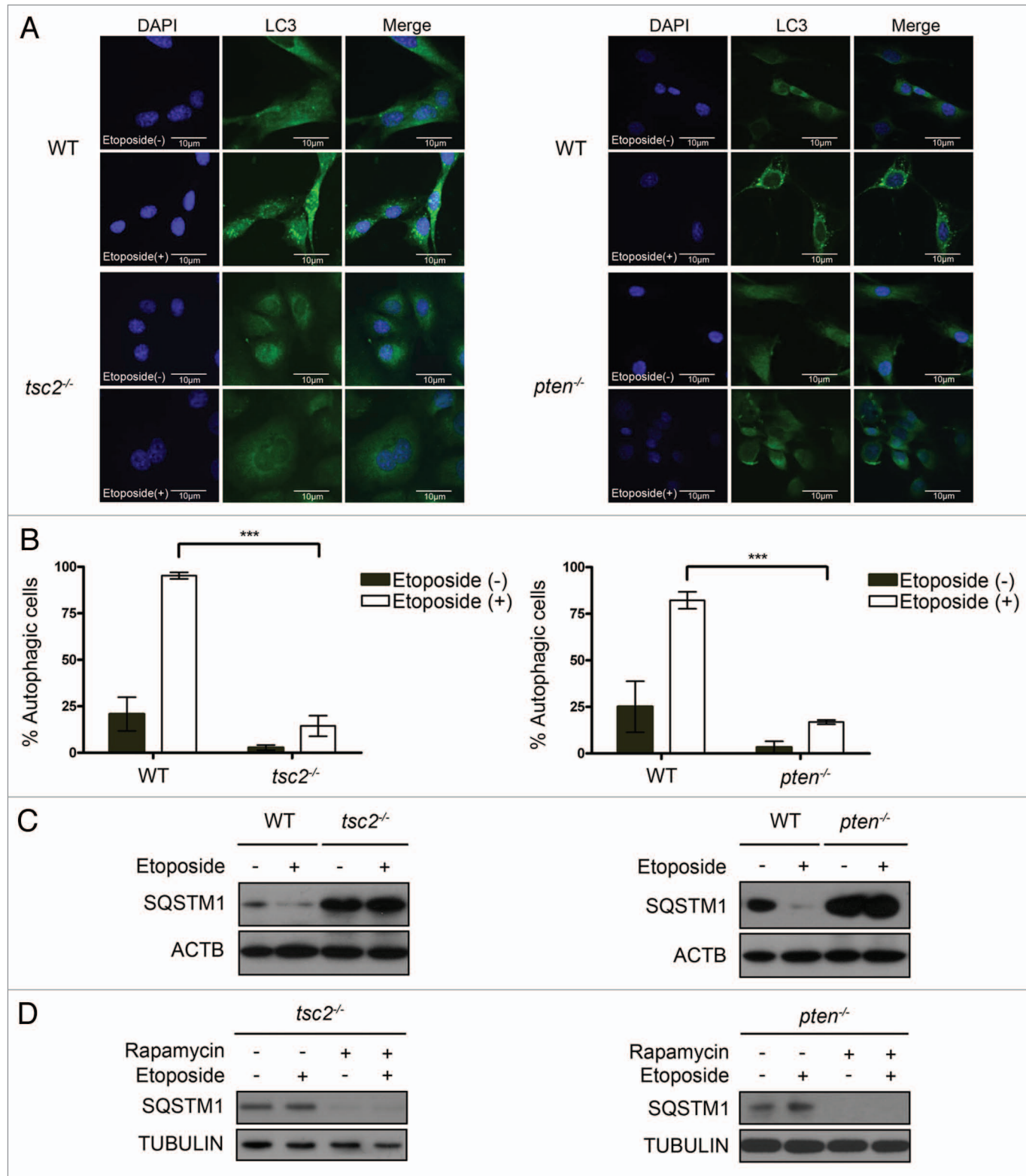


Figure 6. MTOR represses etoposide-induced autophagy. **(A)** Loss of TSC2 or PTEN abrogated etoposide-induced LC3 aggregation. Cells were fixed and stained with anti-LC3 antibody, and the LC3 puncta (green) were visualized with immunofluorescence. DNA was counterstained with DAPI (blue). Representative images are shown. **(B)** Quantification of LC3 puncta-positive cells using a threshold of > 10 dots per cell. More than 200 cells were analyzed. **(C)** Loss of TSC2 or PTEN abrogated degradation of SQSTM1 upon 24 h etoposide treatment. **(D)** Rapamycin induced degradation of SQSTM1 in *tsc2*^{-/-} or *pten*^{-/-} MEFs. Cells pretreated with 10nM rapamycin or left untreated for 6 h and subsequently exposed to etoposide for 24 h were subjected to immunoblotting.

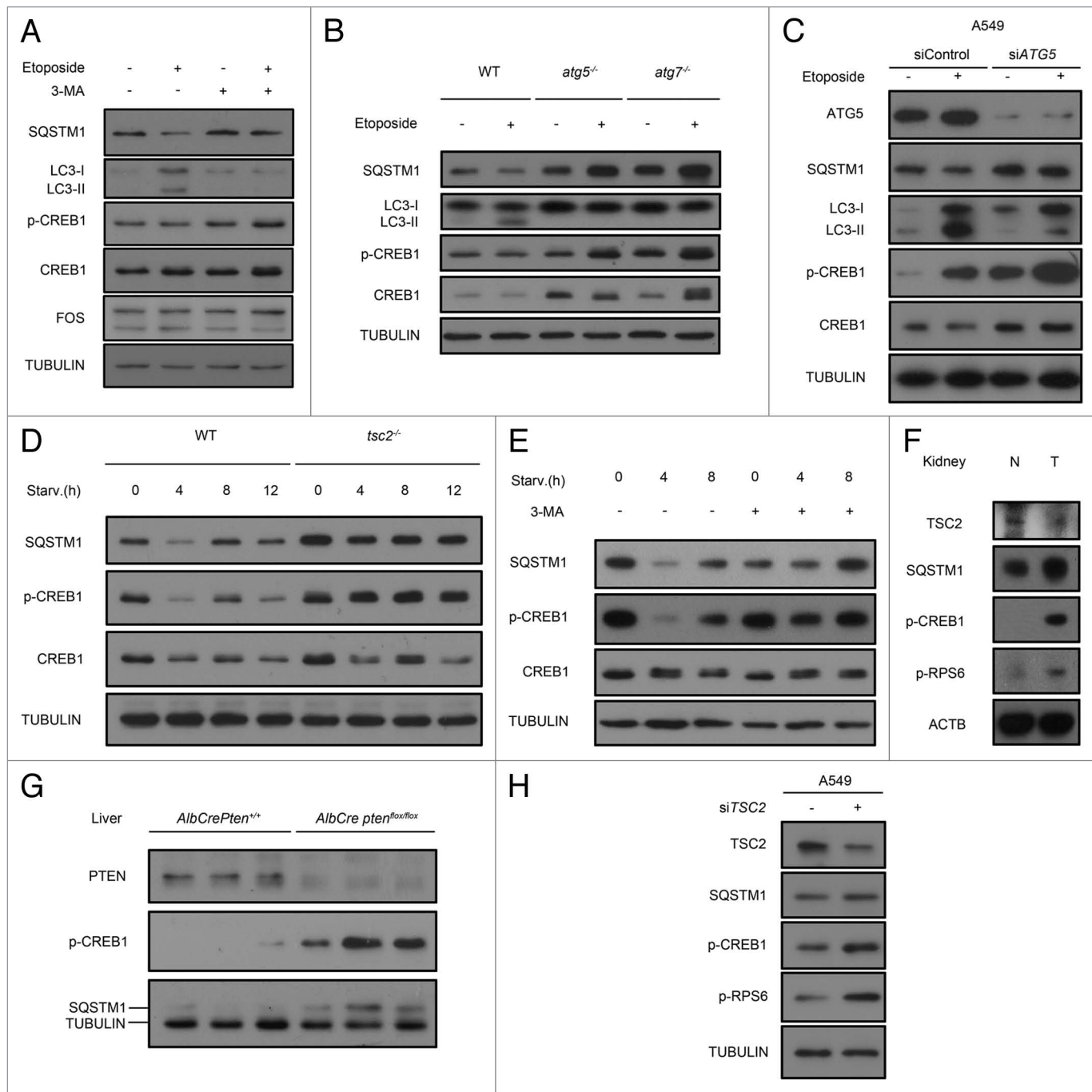


Figure 7. Autophagy suppresses CREB1 activity. Protein samples extracted from cells and tissues were subjected for immunoblotting (**A-H**). (**A**) Inhibition of autophagy boost etoposide-induced CREB1. WT MEFs were treated with either etoposide, 3-MA, or etoposide in combination with 3-MA or left untreated for 24 h. (**B**) Upon etoposide treatment for 24 h, *atg5*^{-/-} or *atg7*^{-/-} MEFs exhibited enhanced CREB1 signaling. (**C**) ATG5 knockdown inhibited autophagy and augments CREB1 phosphorylation and accumulation. A549 cells transfected with nontargeting control siRNA or *ATG5* specific siRNA were subsequently exposed to etoposide for 24 h. (**D**) Fluctuation of CREB1 activity inversely correlated with state of starvation-induced autophagy. WT and *tsc2*^{-/-} MEFs were subjected to starvation (starv.) for the indicated times. (**E**) Inhibition of autophagy reversed starvation suppression of CREB1. WT MEFs subjected to starvation for the indicated times were treated with or without 3-MA. Deficiency in TSC2 (**F**) or PTEN (**G**) led to inhibition of autophagy and enhanced phosphorylation of CREB1 protein in vivo. (**F**) Kidney tumor tissue (T) and adjacent normal kidney tissue (N) from a TSC patient. (**G**) Age- and genetic background-matched livers from three WT (*AlbCrePten*^{+/+}) mice and mutant livers from three *AlbCre pten*^{fl/fl} mice. (**H**) TSC2 knockdown inhibited autophagy and elevates the phosphorylation and accumulation of CREB1. A549 cells were transfected with non-targeting control siRNA or *TSC2*-specific siRNA for 48 h.

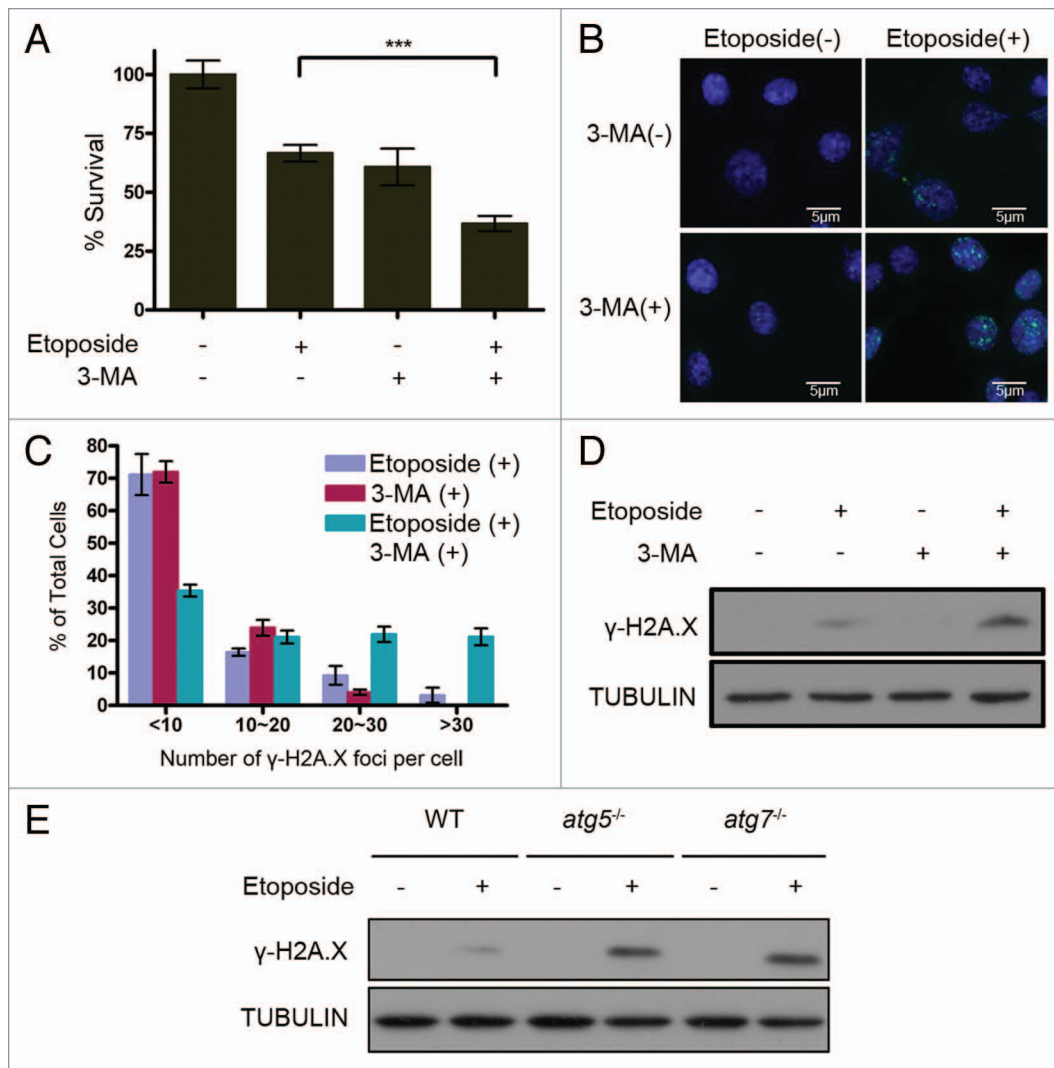


Figure 8. Pharmacological and genetic inhibition of autophagy augments etoposide-induced DNA damage response. WT MEFs were treated with either etoposide, 3-MA, etoposide in combination with 3-MA or left untreated (**A–D**). Autophagy-deficient $atg5^{-/-}$ and $atg7^{-/-}$ MEFs and their counterpart WT cells were subjected to etoposide treatment (**E**). (**A**) Inhibition of autophagy by 3-MA decreased the viability of etoposide treated cells. Cell viability was determined with the MTT assay. ***P < 0.001. (**B**) Inhibition of autophagy by 3-MA enhanced etoposide-induced accumulation of γ -H2A.X foci. Cells were fixed and stained with anti- γ -H2A.X antibody, and the γ -H2A.X foci (green) were subsequently visualized with immunofluorescence. DNA counterstaining was performed using DAPI (blue). Representative images are shown. (**C**) Quantification of the γ -H2A.X foci in more than 200 cells of each treatment group from (**B**). (**D**) Inhibition of autophagy by 3-MA increased etoposide-mediated accumulation of γ -H2A.X protein. (**E**) Increased accumulation of γ -H2A.X protein in etoposide-treated $atg5^{-/-}$ and $atg7^{-/-}$ MEFs.

the mutant mouse livers with hepatocyte-specific *pten* deletion. Increased abundance of SQSTM1 and hyperphosphorylated CREB1 was seen in the mutant liver tissues, compared with that in the liver tissues derived from age- and genetic background-matched WT mice (Fig. 7G). Consistent with those results, TSC2 knockdown increased the abundance of SQSTM1 and the phosphorylation of CREB1 in A549 cells (Fig. 7H).

Suppression of autophagy augments etoposide-induced DNA damage through activation of CREB1

To investigate the effect of autophagy on cell survival and DNA damage, we first measured the cell viability of WT MEFs treated with etoposide in the absence or presence of 3-MA. As observed in Figure 8A, etoposide or 3-MA reduced the cell

viability of WT cells, while the combination of both etoposide and 3-MA induced a marked decrease in the cell viability of WT MEFs. As expected, inhibition of autophagy by 3-MA significantly enhanced etoposide-induced DNA damage in WT MEFs, as evidenced by increased γ -H2A.X foci and γ -H2A.X expression (Fig. 8B–D). Furthermore, $atg5^{-/-}$ and $atg7^{-/-}$ MEFs showed higher expression of γ -H2A.X comparing to WT MEFs under etoposide treatment (Fig. 8E). These results suggest that autophagy protects cells from etoposide-induced DNA damage.

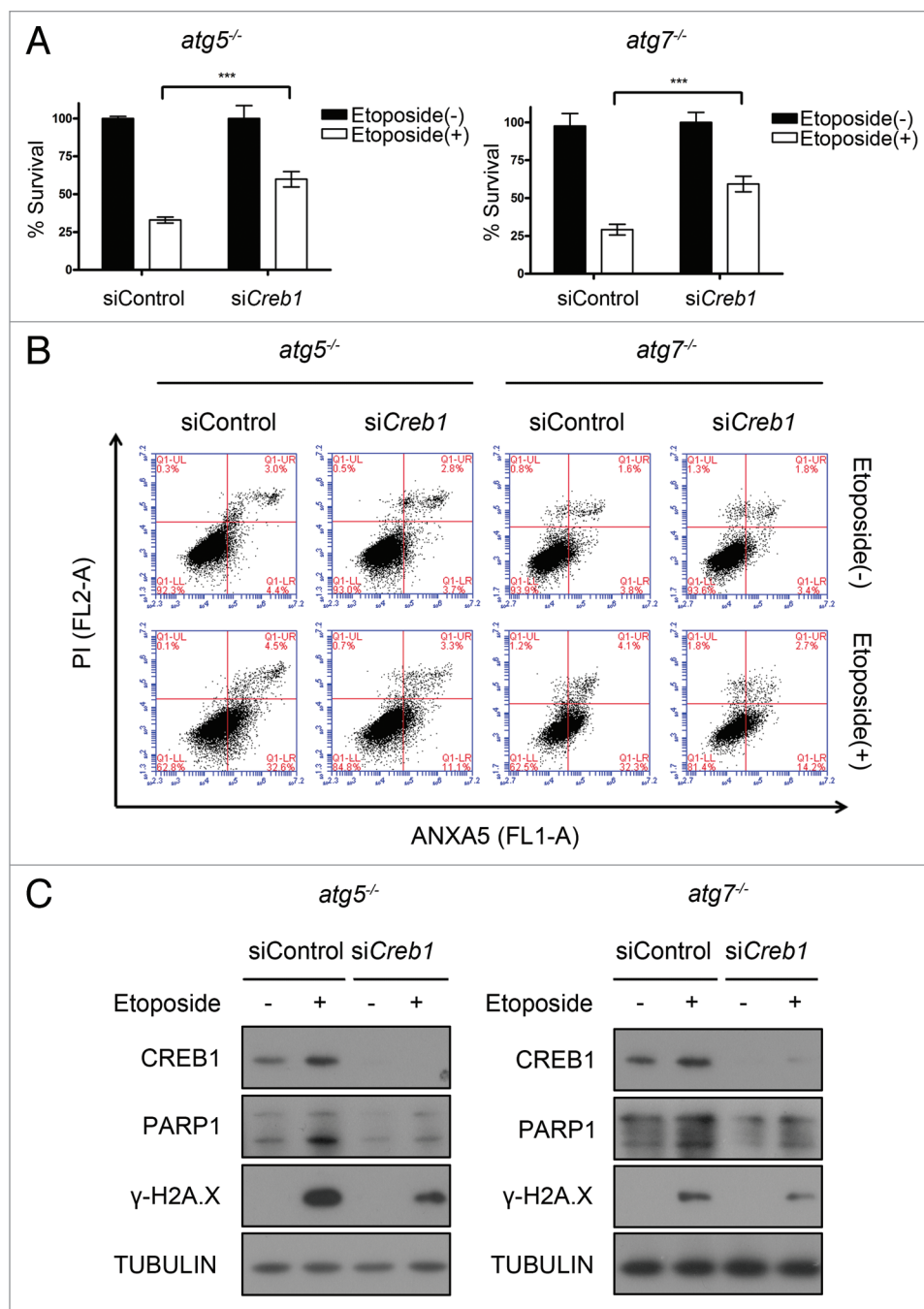
To further investigate the potential role of CREB1 in impaired autophagy-augmented DNA damage and cell death, siRNA-mediated silencing of *Creb1* was performed in $atg5^{-/-}$ and $atg7^{-/-}$ MEFs. As shown in Figure 9A, etoposide-induced cell death of

Figure 9. Autophagy promotes DNA damage-induced apoptosis through CREB1. *atg5*^{-/-} or *atg7*^{-/-} MEFs transfected with nontargeting control siRNA or *Creb1*-specific siRNA were subsequently exposed to etoposide (**A–C**). (**A**) Reduction in CREB1 increased the viability of etoposide-treated *atg5*^{-/-} or *atg7*^{-/-} MEFs. Cell viability was determined with the MTT assay. ***P < 0.001. (**B**) FACS analysis showed that CREB1 knockdown protected cells from etoposide-induced apoptosis. The percentage of cells gated in LR and UR quadrants represents the extent of apoptosis. (**C**) Immunoblotting assay showed that knockdown of CREB1 attenuated the induction of γ-H2A.X protein and PARP1 cleavage in etoposide-treated *atg5*^{-/-} or *atg7*^{-/-} MEFs.

atg5^{-/-} and *atg7*^{-/-} cells was significantly inhibited by suppression of CREB1. In addition, CREB1 knockdown cells treated with etoposide exhibited a lower apoptotic rate comparing to the cells transfected with negative control siRNA (Fig. 9B). As expected, knockdown of CREB1 in *atg5*^{-/-} and *atg7*^{-/-} MEFs was able to block the cleavage of PARP1 and attenuate the DNA damage response as assessed by inhibition of γ-H2A.X induction upon etoposide treatment (Fig. 9C).

Reactivation of CREB1 or inhibition of autophagy alleviates MTOR inhibition-mediated chemoresistance

To elucidate the role of autophagy regulation of CREB1 activity in MTOR inhibition-mediated protective effect on cell survival, we examined the effect of forskolin or 3-MA alone or in combination with etoposide on the cell viability of rapamycin-pretreated MTOR-hyperactivated cells. Preinhibition of MTOR markedly increased the cell viability of MTOR-hyperactivated cells treated with etoposide (Fig. 2A; Fig. 10A). However, forskolin or 3-MA in combination with etoposide greatly reduced the cell viability of MTOR-hyperactivated cells treated with rapamycin, indicating that reactivation of CREB1 or suppression of autophagy can reverse MTOR inhibition-mediated chemoresistance. Furthermore, we found that forskolin or 3-MA alone significantly reduced the cell viability of MTOR-hyperactivated cells pretreated with rapamycin, suggesting that reactivation of CREB1 or suppression of autophagy can enhance the efficacy of rapamycin. This result suggests that autophagy suppression of CREB1 activity is responsible for MTOR inhibition-mediated chemoresistance.



Discussion

Tumor chemoresistance is an important contributor to the failure of cancer therapy. By inhibiting MTOR signaling pathway, rapamycin is emerging as an effective anticancer drug. However, recent data, including ours presented here, have implicated MTOR inhibition in chemoresistance, as rapamycin renders cells refractory to chemotherapy. In this study, we have identified that MTOR activates CREB1 through suppression of autophagy. CREB1 activation due to impaired autophagy sensitizes MTOR-hyperactivated cells to etoposide-induced genomic damage and subsequent apoptosis. Suppression of CREB1 by

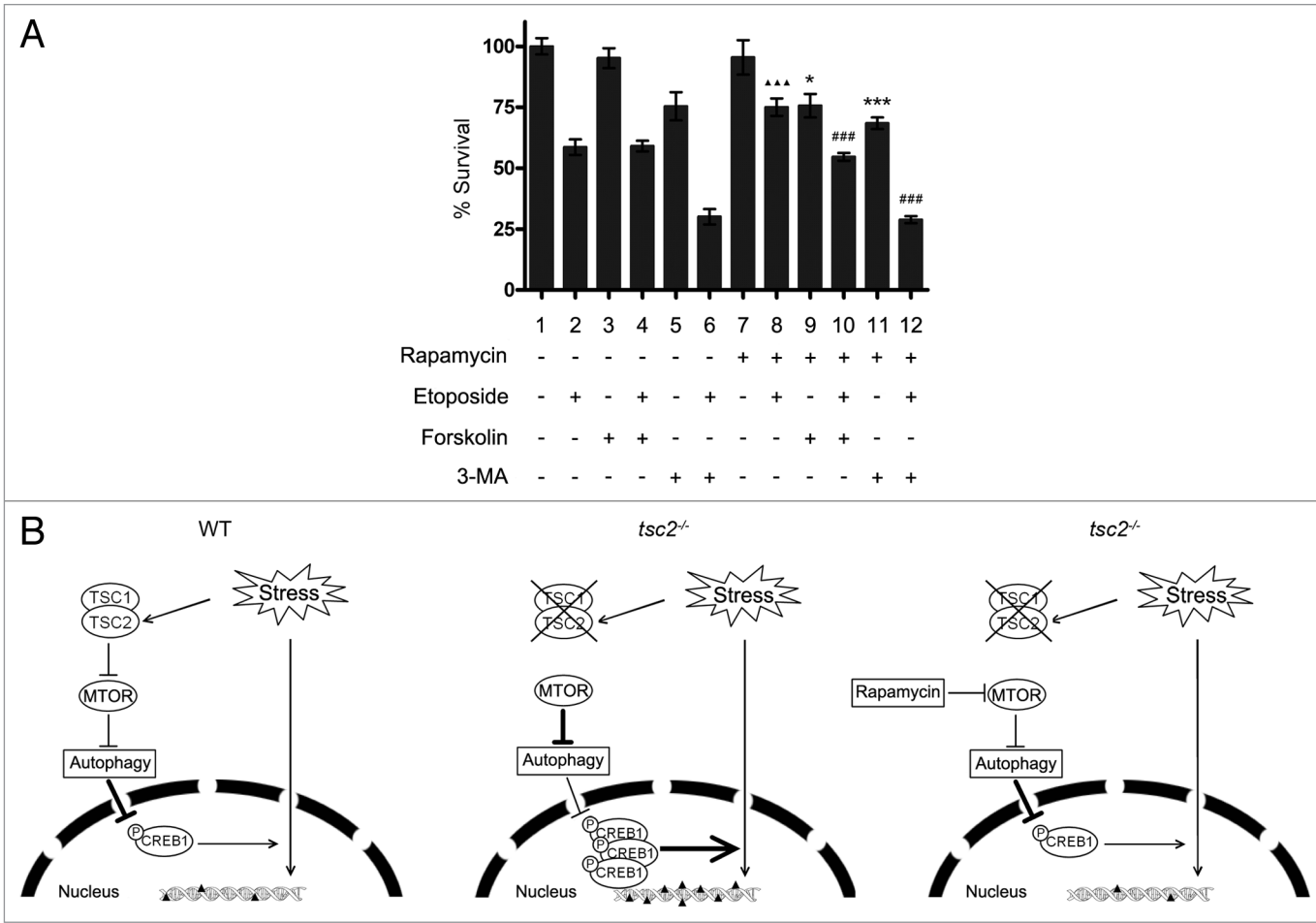


Figure 10. Reactivation of CREB1 alleviates MTOR inhibition-mediated chemoresistance. **(A)** Reactivation of CREB1 by forskolin or inhibition of autophagy by 3-MA reduced the viability of 10 nM rapamycin pretreated-MTOR-hyperactivated cells with or without etoposide treatment. Cell viability was determined with the MTT assay. Data are shown as the mean \pm s.d. of three replicates and are representative of three independent experiments. Comparison of column 9 and 11 with column 7, column 10 and 12 with column 8, and column 8 with column 2 (* $P < 0.05$; ** $P < 0.001$; # $P < 0.001$ or ▲▲▲ represent $P < 0.001$). **(B)** Diagrammatic illustration for regulation of CREB1 by MTOR-related autophagy signaling in modulating stress-induced DNA damage in WT, *tsc2*^{-/-}, or *tsc2*^{-/-} MEFs treated with rapamycin. The dark triangles represent DSBs. The thickness of the lines represents the intensity of the effects.

activated autophagy attenuates etoposide-induced DNA damage and underlies rapamycin-mediated chemoresistance (Fig. 10B). Inhibition of autophagy or potentiation of CREB1 may therefore become a novel regimen in synergizing the effect of chemotherapy in the treatment of cancer.

By integrating a wide range of signals, including nutrients, growth factors, and stress conditions, MTOR regulates a variety of cellular processes. Under DNA damage-induced stress conditions, MTOR activity can be regulated through an AMPK-TSC2 dependent mechanism.⁵⁶ However the effectors downstream of MTOR and their roles in DNA damage-induced stress response remain largely elusive. In the present study, we show that MTOR suppressor TSC2- or PTEN-deficient MEFs exhibited enhanced CREB1 activation under either etoposide or cisplatin induced genotoxic stress condition. Furthermore, suppression of MTOR by either rapamycin or siRNA silencing inhibited the response of CREB1 and its target gene FOS to genotoxic stress in TSC2- or PTEN-deficient MEFs and tumor cell lines. The CREB1 activation is thus dependent on MTOR signaling.

CREB1 functions as a nuclear transcription factor and is regulated by multiple protein kinases and protein phosphatases. Recently, it has been shown that CREB1 can be degraded through the proteasome pathway.^{57,58} Besides the ubiquitination-dependent proteasomal degradation system, autophagy is another major intracellular protein degradation system that is important for the turnover of cytoplasmic proteins and organelles.^{59,60} We found that the autophagy induction is impaired in MTOR-hyperactivated MEFs and CREB1 activity is negatively regulated by autophagy. Both the pharmacological and genetic suppressions of autophagy were able to stimulate the phosphorylation and accumulation of CREB1 under the conditions of two autophagy stimuli, chemotherapy and nutrient starvation, respectively. Therefore the status of autophagy dictates the magnitude of CREB1 activation by chemotherapeutics. Furthermore, an inverse correlation between autophagy activity and CREB1 activity in vivo was presented in the kidney tumor tissue obtained from a TSC patient and the liver tissues derived from the mice with hepatocyte-specific *pten* deletion. Although

we have uncovered autophagy suppression of CREB1, its underlying regulatory mechanism is yet to be elucidated.

CREB1 is a critical cell signaling node regulating cell proliferation, apoptosis, and other cellular responses. In this study, we found that suppression of CREB1 inhibited etoposide-induced apoptosis and increased the cell viability in MTOR-hyperactivated cells. On the other hand, stimulation of cAMP and CREB1 signaling enhanced DNA damage-induced apoptosis and inhibited the cell viability in WT MEFs. Furthermore, reactivation of cAMP and CREB1 signaling significantly suppressed the viability of rapamycin-pretreated MTOR-hyperactivated MEFs. These results suggest that aberrant MTOR hyperactivation sensitizes cells to DNA damage-induced apoptotic cell death through sustained CREB1 activation.

Although the elevation of autophagy activity has been observed in cancer cells treated with chemotherapy, the role of autophagy activation in chemotherapy causes considerable controversy. Here, we present that the induced autophagy represents a protective role in WT MEFs as inhibition of autophagy enhanced etoposide-induced DNA damage and reduced the cell viability. Consistent with the observation from Henske's group,⁶¹ inhibition of autophagy significantly suppressed the viability of rapamycin-pretreated MTOR-hyperactivated MEFs.

Even though it is known that defective autophagy leads to increased genomic damage, the mechanism underlying this connection is not yet identified. Accumulation of malfunctioning intracellular structures and noxious protein aggregates due to autophagy impairment may contribute to induction of genome damage.⁶² Our data demonstrate that impaired autophagy due to genetic depletion of autophagy-related genes promoted etoposide-induced DNA damage response through accumulation of activated CREB1, as suppression of CREB1 reduced DNA damage, inhibited apoptosis, and increased cell survival. It remains to be determined how CREB1 mediates etoposide-induced DNA damage and apoptotic cell death. MTOR is a positive regulator of *CCND1* expression.^{63–65} *CCND1*, a well-known target gene of CREB1,⁴⁵ functions in amplifying the cellular DNA damage.⁶⁶ Therefore we speculate that MTOR suppresses autophagy which in turn unleashes its inhibitory effect on CREB1 function. The potentiated CREB1 then stimulates *CCND1* expression and increases DNA damage.

In conclusion, our results not only reveal an important role for MTOR modulation of autophagy signaling in regulating CREB1 activity, but also elucidate the role of the hyperactive CREB1 induced by an autophagy inhibition in the regulation of cell viability and etoposide-induced DNA damage response. CREB1 inducers as well as autophagy inhibitors thus can be seen as potential enhancers of chemotherapeutics in cancer treatment. Further elucidation of how autophagy signaling regulates CREB1 activity may lead to the identification of novel targets for the treatment of cancers driven by aberrant activation of MTOR signaling.

Materials and Methods

Reagents, antibodies, and plasmids

Rapamycin (R0395), etoposide (E1383), 3-MA (08592), forskolin (F6886), baflomycin A₁ (B1793), saponin (S4521),

3-[4, 5-dimethyl-thiazol-2yl] 2, 5-diphenyltetrazoliumbromide (MTT) (88417), and 4', 6'-diamidino-2-phenylindole (DAPI) (D9542) were purchased from Sigma-Aldrich. Cisplatin was from DBL, Hospira. Lipofectamine 2000 (11668-019) was obtained from Invitrogen. DMEM (SH30022.01B) and FBS (SV30087.02) were from HyClone. Dimethyl sulfoxide (DMSO) (0231) was from Amresco. Chemiluminescence (NC15079) was from Thermo Scientific. Antibodies were from Cell Signaling [anti-PARP1 (9542), anti-PTEN (9559), anti- γ -H2A.X (2577), anti-phospho-CREB1 (Ser133) (9198), anti-CREB1 (9197), and anti-ATG7 (8558)], Novus Biologicals [anti-ATG5 (NB110-53818)], MBL [anti-SQSTM1 (PM045) and anti-LC3 (PM036)], and Santa Cruz Biotechnology [anti-FOS/c-FOS (sc-52), anti-TSC2 (sc-893), anti-ACTB/ β -ACTIN (sc-8432), anti-TUBULIN (sc-12462), FITC-conjugated goat anti-rabbit (sc-2012), HRP-labeled goat anti-mouse (sc-2005), and HRP-labeled goat anti-rabbit (sc2004)]. Anti-phospho-RPS6/S6 (Ser235/236) has been described previously.⁶⁷ Gal4CREB (M1-CREB1) plasmid was a generous gift from Michael Greenberg (Harvard Medical School). pLXIN-hyg-M1-CREB1 was generated by the insertion of a XhoI and BglII digested PCR product of Gal4CREB plasmid using primers 5'-CTCGGATCCA CCATGACCAT GGAATCTGGA-3' and 5'-GCGCTCGAGA TCTGATTGT GGCAGTAAA-3' into a modified pLXIN retroviral vector with a hygromycin resistance gene (pLXIN-hyg).⁶⁸

Cell culture

Immortalized *tsc2*^{-/-}, *pten*^{-/-} MEFs and control MEF lines as well as TSC2-deficient rat ELT-3 cells have been described previously.^{8,67,69,70} Immortalized *atg5*^{-/-} MEFs were generated by Noboru Mizushima (Tokyo Medical and Dental University) and immortalized *atg7*^{-/-} MEFs were generated by Masaaki Komatsu (Tokyo Metropolitan Institute Medical Science). Human A549, MCF7, and MDA-MB-468 cell lines were from American Type Culture Collection. ELT-3 cells were maintained and propagated in Dulbecco's modified Eagle's medium (DMEM)/F12 (1:1) with 10% fetal bovine serum. The other cell lines used in this study were maintained in DMEM medium supplemented with 10% FBS and 1% antibiotics in a 37 °C humidified incubator containing 5% CO₂. Production of retroviruses and subsequent generation of stable gene expression cell lines were described elsewhere.²

RNA interference

The siRNAs and their controls were synthesized by Shanghai GenePharma. Cells were seeded in 6-well plates and transfected with siRNAs using Lipofectamine 2000 for 48 h following the manufacturer's instructions. siRNA targeted sequences were as follows: negative control: 5'-TTCTCCGAAC GTGTCACGT-3'; mouse and rat *Creb1*: 5'- GGAGTCTGTG GATACTGTA -3';⁷¹ mouse *Mtor*: 5'-GAACTCGCTG ATCCAGATG-3'; human *ATG5*: 5'- GGACGAATT CAACTTGTT -3'; human *TSC2*: 5'-CAATGAGTCA CAGTCCTTGA -3'.⁷²

Cell viability assay

MEFs were plated at 3,000 cells per well in a 96-well tissue culture plate. The next day, cells were treated with 0.4 μ M etoposide alone, or in combination with 5 mM 3-MA or 50 μ M forskolin as described for the indicated time. After a 2-d culture

period, an MTT solution was added to a final concentration of 0.5 mg/ml. After 4 h, the colored formazan crystals were dissolved in 150 μ l of DMSO, and optical densities were read using a microplate reader at 490 nm. The absorbance at 490 nm directly corresponds with cell number. The viability ratio was defined as OD value of the sample/OD value of control \times 100%. Each data point is the average of results from 5 wells from each of three independent experiments.

Flow cytometry analysis

After treatment of cells with 0.4 μ M etoposide for 24 h, cells were analyzed for apoptosis using an ANXA5-FITC and PI apoptosis assay kit (Neobioscience, FAK011) according to the manufacturer's protocol. Briefly, 1×10^6 cells were collected, washed twice with PBS, and incubated with ANXA5-FITC and PI for 15 min at room temperature in the dark. Cells were then immediately analyzed with the BD Accuri C6 flow cytometer (BD Biosciences). The combination of ANXA5-FITC and PI allows for the differentiation among viable (ANXA5-FITC negative, PI negative), early apoptotic (ANXA5-FITC positive, PI negative), late apoptotic and necrotic (ANXA5-FITC positive, PI positive) cells.

Quantitative real-time RT-PCR analysis

Total RNA was extracted from cells using Trizol reagent (Invitrogen, 15596-018) and reversely transcribed using the PrimeScript RT Reagent Kit (TaKaRa, DRR037A). cDNA was used as a template in a quantitative PCR reaction. Amplification was done for 40 cycles using TransStart Green qPCR SuperMix (TransGen Biotech, AQ131-03). Oligonucleotide primers were synthesized to detect *Fos* with *Actb* as internal control. Primers were synthesized by Sangon Biological Engineering Technology & Services. The primer sequences were as follows: mouse *Fos* forward: 5'-ATGGGCTCTC CTGTCAACAC-3', mouse *Fos* reverse: 5'-ACGGAGGAGA CCAGAGTGG-3'; mouse *Actb* forward: 5'-AGAGGGAAAT CGTGCCTGAC-3', mouse *Actb* reverse: 5'-CAATACTGAT GACCTGGCCGT-3'.

Autophagy analysis

For autophagy stimulation, cells were washed 3 times with PBS and incubated for indicated times in starvation medium (DMEM medium without serum and glutamine) (Invitrogen, 11960) or complete medium containing 0.4 μ M etoposide in a 37 °C humidified incubator containing 5% CO₂. Autophagy was assessed by endogenous LC3 redistribution, LC3 conversion from LC3-I to LC3-II and SQSTM1 degradation. To inhibit starvation- or chemotherapeutics-induced autophagy, cells were treated with 5 mM 3-MA in starvation medium or complete medium, or with baflomycin A₁ (100 ng/ml) in complete medium.

Immunofluorescence assay

Cells were cultured on glass coverslips prior to immunofluorescence analysis. After treatment of cells with indicated drugs for 24 h, cells were washed 3 times with PBS, fixed in 4% paraformaldehyde for 10 min and permeabilized in PBS containing 0.1% saponin for 10 min. After being washed with PBS and blocked with normal goat serum for 30 min, the cells were stained with primary antibodies (anti- γ -H2A.X for endogenous γ -H2A.X; anti-LC3 for endogenous LC3) in blocking buffer for 1 h, followed by washes 3 times with PBS and incubated with FITC-conjugated goat anti-rabbit secondary antibody in blocking buffer for 1 h.

Nuclear counterstaining with DAPI was performed after removal of excess secondary antibody. All procedures were conducted at room temperature. Confocal laser scanning of fixed cells was performed on a confocal microscope (Ultraview vox.; PerkinElmer) equipped with a camera (Hamamatsu, C9100-13) using an Olympus APON 60 \times 1.49 NA objective. FITC and DAPI images were taken and overlapped using velocity software (PerkinElmer).

Immunoblotting

For immunoblotting, cells were washed 3 times with PBS and harvested on ice with lysis buffer (2% SDS, 0.1 M DTT, 60 mM Tris pH 6.8, 10% glycerol). Whole cell lysates were resolved by SDS-PAGE. Proteins were subsequently transferred onto PVDF membrane (Millipore, IPVH00010) and blocked for 1 h at room temperature in PBS containing 0.2% Tween-20 (PBST) and 5% nonfat dry milk and immunoblotted with the indicated antibodies in PBST with 5% nonfat dry milk, followed by the incubation with HRP-labeled secondary antibodies and the detection by chemiluminescence.

Human kidney tumor assessment

Kidney angiomyolipomas and its adjacent normal kidney tissue from a TSC patient with a *TSC2* mutation (g.10059delC, p.S132SfsX50) were freshly dissected, sonicated, and extracted with lysis buffer for immunoblotting.⁷⁰ All the procedures were performed under the permission of the Peking Union Medical College Hospital Ethics Board.

Assessment of mouse livers with hepatocyte pten deletion

To generate mice with hepatocyte-specific *pten* deletion, we crossed *Pten*^{fl/fl} mice with *AlbCre* transgenic mice.⁷³ For immunoblotting, the liver tissues from 3 WT-mice (*AlbCrePten*^{+/+}, 9 mo-old) and the liver tissues from 3 homozygous *Pten* exons 4 and 5 deletion mice (*AlbCre pten*^{fl/fl}, 9 mo-old) were sonicated and extracted with lysis buffer. All animal experiments were approved by the Animal Research Committee, Institute of Laboratory Animals, and Chinese Academy of Medical Sciences & Peking Union Medical College.

Statistical analysis

For immunofluorescence assay, all values are reported as mean \pm s.d. from 3 independent experiments. For the MTT assay, data are shown as the mean \pm s.d. of 5 replicates and are representative of 3 independent experiments. Differences were analyzed with the 2-tailed Student *t*-test with GraphPad Prism 5 software and *P* < 0.05 considered statistically significant.

Disclosure of Potential Conflicts of Interest

No potential conflicts of interest needed to be disclosed.

Acknowledgments

We thank Na Mi and Li Yu (School of Life Science, Tsinghua University) for instruction on autophagy analysis. This work was supported by the National Basic Research Program of China (973 Program: 2009CB522203), the Ministry of Science and Technology Key Program (2013ZX10002008-004), the National Natural Science Foundation of China (Grant: 81130085), the Research Fund for the Doctoral Program of Higher Education of China (200800230022) and the Ministry of Education of China 111 Project (B08007).

Supplemental Materials

Supplemental materials may be found here:

www.landesbioscience.com/journals/autophagy/article/26447

References

1. Schmelzle T, Hall MN. TOR, a central controller of cell growth. *Cell* 2000; 103:253-62; PMID:11057898; [http://dx.doi.org/10.1016/S0092-8674\(00\)00117-3](http://dx.doi.org/10.1016/S0092-8674(00)00117-3)
2. Ma J, Meng Y, Kwiatkowski DJ, Chen X, Peng H, Sun Q, Zha X, Wang F, Wang Y, Jing Y, et al. Mammalian target of rapamycin regulates murine and human cell differentiation through STAT3/p63/Jagged/Notch cascade. *J Clin Invest* 2010; 120:103-14; PMID:20038814; <http://dx.doi.org/10.1172/JCI37964>
3. Sun Q, Chen X, Ma J, Peng H, Wang F, Zha X, Wang Y, Jing Y, Yang H, Chen R, et al. Mammalian target of rapamycin up-regulation of pyruvate kinase isoenzyme type M2 is critical for aerobic glycolysis and tumor growth. *Proc Natl Acad Sci U S A* 2011; 108:4129-34; PMID:21325052; <http://dx.doi.org/10.1073/pnas.1014769108>
4. Noda T, Ohsumi Y. Tor, a phosphatidylinositol kinase homologue, controls autophagy in yeast. *J Biol Chem* 1998; 273:3963-6; PMID:9461583; <http://dx.doi.org/10.1074/jbc.273.7.3963>
5. Hollander MC, Blumenthal GM, Dennis PA. PTEN loss in the continuum of common cancers, rare syndromes and mouse models. *Nat Rev Cancer* 2011; 11:289-301; PMID:21430697; <http://dx.doi.org/10.1038/nrc3037>
6. Tee AR, Manning BD, Roux PP, Cantley LC, Blenis J. Tuberous sclerosis complex gene products, Tuberin and Hamartin, control mTOR signaling by acting as a GTPase-activating protein complex toward Rheb. *Curr Biol* 2003; 13:1259-68; PMID:12906785; [http://dx.doi.org/10.1016/S0960-9822\(03\)00506-2](http://dx.doi.org/10.1016/S0960-9822(03)00506-2)
7. Inoki K, Li Y, Zhu T, Wu J, Guan KL. TSC2 is phosphorylated and inhibited by Akt and suppresses mTOR signalling. *Nat Cell Biol* 2002; 4:648-57; PMID:12172553; <http://dx.doi.org/10.1038/ncb839>
8. Kwiatkowski DJ, Zhang H, Bandura JL, Heiberger KM, Glogauer M, el-Hasemite N, Onda H. A mouse model of TSC1 reveals sex-dependent lethality from liver hemangiomas, and up-regulation of p70S6 kinase activity in Tsc1 null cells. *Hum Mol Genet* 2002; 11:525-34; PMID:11875047; <http://dx.doi.org/10.1093/hmg/11.5.525>
9. Potter CJ, Pedraza LG, Xu T. Akt regulates growth by directly phosphorylating Tsc2. *Nat Cell Biol* 2002; 4:658-65; PMID:12172554; <http://dx.doi.org/10.1038/ncb840>
10. Gao X, Zhang Y, Arrazola P, Hino O, Kobayashi T, Yeung RS, Ru B, Pan D. Tsc tumour suppressor proteins antagonize amino-acid-TOR signalling. *Nat Cell Biol* 2002; 4:699-704; PMID:12172555; <http://dx.doi.org/10.1038/ncb847>
11. Manning BD, Tee AR, Logsdon MN, Blenis J, Cantley LC. Identification of the tuberous sclerosis complex-2 tumor suppressor gene product tuberin as a target of the phosphoinositide 3-kinase/akt pathway. *Mol Cell* 2002; 10:151-62; PMID:12150915; [http://dx.doi.org/10.1016/S1097-2765\(02\)00568-3](http://dx.doi.org/10.1016/S1097-2765(02)00568-3)
12. Shaw RJ, Bardeesy N, Manning BD, Lopez L, Kosmatka M, DePinho RA, Cantley LC. The LKB1 tumor suppressor negatively regulates mTOR signalling. *Cancer Cell* 2004; 6:91-9; PMID:15261145; <http://dx.doi.org/10.1016/j.ccr.2004.06.007>
13. Zoncu R, Efeyan A, Sabatini DM. mTOR: from growth signal integration to cancer, diabetes and ageing. *Nat Rev Mol Cell Biol* 2011; 12:21-35; PMID:21157483; <http://dx.doi.org/10.1038/nrm3025>
14. Guertin DA, Sabatini DM. Defining the role of mTOR in cancer. *Cancer Cell* 2007; 12:9-22; PMID:17613433; <http://dx.doi.org/10.1016/j.ccr.2007.05.008>
15. Garcia-Echeverria C. Blocking the mTOR pathway: a drug discovery perspective. *Biochem Soc Trans* 2011; 39:451-5; PMID:21428918; <http://dx.doi.org/10.1042/BST0390451>
16. Lee CH, Inoki K, Karbowniczek M, Petroulakis E, Sonenberg N, Henske EP, Guan KL. Constitutive mTOR activation in TSC mutants sensitizes cells to energy starvation and genomic damage via p53. *EMBO J* 2007; 26:4812-23; PMID:17962806; <http://dx.doi.org/10.1038/sj.emboj.7601900>
17. Ghosh S, Tergaonkar V, Rothlin CV, Correa RG, Bottero V, Bist P, Verma IM, Hunter T. Essential role of tuberous sclerosis genes TSC1 and TSC2 in NF-kappaB activation and cell survival. *Cancer Cell* 2006; 10:215-26; PMID:16959613; <http://dx.doi.org/10.1016/j.ccr.2006.08.007>
18. Ozcan U, Ozcan L, Yilmaz E, Duvel K, Sahin M, Manning BD, Hotamisligil GS. Loss of the tuberous sclerosis complex tumor suppressors triggers the unfolded protein response to regulate insulin signaling and apoptosis. *Mol Cell* 2008; 29:541-51; PMID:18342602; <http://dx.doi.org/10.1016/j.molcel.2007.12.023>
19. Chaturvedi D, Gao X, Cohen MS, Taunton J, Patel TB. Rapamycin induces transactivation of the EGFR and increases cell survival. *Oncogene* 2009; 28:1187-96; PMID:19151764; <http://dx.doi.org/10.1038/onc.2008.490>
20. Gonzalez GA, Montminy MR. Cyclic AMP stimulates somatostatin gene transcription by phosphorylation of CREB at serine 133. *Cell* 1989; 59:675-80; PMID:2573431; [http://dx.doi.org/10.1016/0092-8674\(89\)90013-5](http://dx.doi.org/10.1016/0092-8674(89)90013-5)
21. Mayr B, Montminy M. Transcriptional regulation by the phosphorylation-dependent factor CREB. *Nat Rev Mol Cell Biol* 2001; 2:599-609; PMID:11483993; <http://dx.doi.org/10.1038/35085056>
22. Shankar DB, Cheng JC, Kinjo K, Federman N, Moore TB, Gill A, Rao NP, Landaw EM, Sakamoto KM. The role of CREB as a proto-oncogene in hematopoiesis and in acute myeloid leukemia. *Cancer Cell* 2005; 7:351-62; PMID:15837624; <http://dx.doi.org/10.1016/j.ccr.2005.02.018>
23. Crans-Vargas HN, Landaw EM, Bhatia S, Sandusky G, Moore TB, Sakamoto KM. Expression of cyclic adenosine monophosphate response-element binding protein in acute leukemia. *Blood* 2002; 99:2617-9; PMID:11895805; <http://dx.doi.org/10.1182/blood.V99.7.2617>
24. Chhabra A, Fernando H, Watkins G, Mansel RE, Jiang WG. Expression of transcription factor CREB1 in human breast cancer and its correlation with prognosis. *Oncol Rep* 2007; 18:953-8; PMID:17786359
25. Seo HS, Liu DD, Bekele BN, Kim MK, Pisters K, Lippman SM, Wistuba II, Koo JS. Cyclic AMP response element-binding protein overexpression: a feature associated with negative prognosis in never smokers with non-small cell lung cancer. *Cancer Res* 2008; 68:6065-73; PMID:18676828; <http://dx.doi.org/10.1158/0008-5472.CAN-07-5376>
26. Linnerth NM, Greenaway JB, Petrik JJ, Moorehead RA. cAMP response element-binding protein is expressed at high levels in human ovarian adenocarcinoma and regulates ovarian tumor cell proliferation. *Int J Gynecol Cancer* 2008; 18:1248-57; PMID:18554190; <http://dx.doi.org/10.1111/j.1525-1438.2007.01177.x>
27. Wu D, Zhau HE, Huang WC, Iqbal S, Habib FK, Sartor O, Cvitanovic L, Marshall FF, Xu Z, Chung LW. cAMP-responsive element-binding protein regulates vascular endothelial growth factor expression: implication in human prostate cancer bone metastasis. *Oncogene* 2007; 26:5070-7; PMID:17310988; <http://dx.doi.org/10.1038/sj.onc.1210316>
28. Yokozaki H, Tortora G, Pepe S, Maronde E, Genieser HG, Jastorff B, Cho-Chung YS. Unhydrolyzable analogues of adenosine 3':5'-monophosphate demonstrating growth inhibition and differentiation in human cancer cells. *Cancer Res* 1992; 52:2504-8; PMID:1314695
29. Marquette A, André J, Bagot M, Bensusan A, Dumaz N. ERK and PDE4 cooperate to induce RAF isoform switching in melanoma. *Nat Struct Mol Biol* 2011; 18:584-91; PMID:21478863; <http://dx.doi.org/10.1038/nsmb.2222>
30. Arnould T, Vankoningsloo S, Renard P, Houbion A, Ninane N, Demazy C, Remacle J, Raes M. CREB activation induced by mitochondrial dysfunction is a new signaling pathway that impairs cell proliferation. *EMBO J* 2002; 21:53-63; PMID:11782425; <http://dx.doi.org/10.1093/emboj/21.1.53>
31. Levine B, Klionsky DJ. Development by self-digestion: molecular mechanisms and biological functions of autophagy. *Dev Cell* 2004; 6:463-77; PMID:15068787; [http://dx.doi.org/10.1016/S1534-5807\(04\)00099-1](http://dx.doi.org/10.1016/S1534-5807(04)00099-1)
32. Mizushima N. Physiological functions of autophagy. *Curr Top Microbiol Immunol* 2009; 335:71-84; PMID:19802560; http://dx.doi.org/10.1007/978-3-642-00302-8_3
33. Ma J, Sun Q, Mi R, Zhang H. Avian influenza A virus H5N1 causes autophagy-mediated cell death through suppression of mTOR signaling. *J Genet Genomics* 2011; 38:533-7; PMID:22133684; <http://dx.doi.org/10.1016/j.jgg.2011.10.002>
34. Kanazawa T, Germano IM, Komata T, Ito H, Kondo Y, Kondo S. Role of autophagy in temozolomide-induced cytotoxicity for malignant glioma cells. *Cell Death Differ* 2004; 11:448-57; PMID:14713959; <http://dx.doi.org/10.1038/sj.cdd.4401359>
35. Harhaji-Trajkovic L, Vilimovich U, Kravice-Stevovic T, Bumbasirevic V, Trajkovic V. AMPK-mediated autophagy inhibits apoptosis in cisplatin-treated tumour cells. *J Cell Mol Med* 2009; 13(9B):3644-54; PMID:20196784; <http://dx.doi.org/10.1111/j.1582-4934.2009.00663.x>
36. Ding ZB, Hu B, Shi YH, Zhou J, Peng YF, Gu CY, Yang H, Shi GM, Ke AW, Wang XY, et al. Autophagy activation in hepatocellular carcinoma contributes to the tolerance of oxaliplatin via reactive oxygen species modulation. *Clin Cancer Res* 2011; 17:6229-38; PMID:21825039; <http://dx.doi.org/10.1158/1078-0432.CCR-11-0816>
37. Soldani C, Scovassi AI. Poly(ADP-ribose) polymerase-1 cleavage during apoptosis: an update. *Apoptosis* 2002; 7:321-8; PMID:12101391; <http://dx.doi.org/10.1023/A:1016119328968>
38. Kuo LJ, Yang LX. Gamma-H2AX - a novel biomarker for DNA double-strand breaks. *In Vivo* 2008; 22:305-9; PMID:18610740
39. Shaw RJ, Lamia KA, Vasquez D, Koo SH, Bardeesy N, Depinho RA, Montminy M, Cantley LC. The kinase LKB1 mediates glucose homeostasis in liver and therapeutic effects of metformin. *Science* 2005; 310:1642-6; PMID:16308421; <http://dx.doi.org/10.1126/science.1120781>

40. Katoh Y, Takemori H, Lin XZ, Tamura M, Muraoka M, Satoh T, Tsuchiya Y, Min L, Doi J, Miyachi A, et al. Silencing the constitutive active transcription factor CREB by the LKB1-SIK signaling cascade. *FEBS J* 2006; 273:2730-48; PMID:16817901; <http://dx.doi.org/10.1111/j.1742-4658.2006.05291.x>
41. Howe SR, Gottardis MM, Everitt JI, Goldsworthy TL, Wolf DC, Walker C. Rodent model of reproductive tract leiomyomata. Establishment and characterization of tumor-derived cell lines. *Am J Pathol* 1995; 146:1568-79; PMID:7539981
42. Kobayashi T, Hirayama Y, Kobayashi E, Kubo Y, Hino O. A germline insertion in the tuberous sclerosis (Tsc2) gene gives rise to the Eker rat model of dominantly inherited cancer. *Nat Genet* 1995; 9:70-4; PMID:7704028; <http://dx.doi.org/10.1038/ng0195-70>
43. Ginty DD, Bonni A, Greenberg ME. Nerve growth factor activates a Ras-dependent protein kinase that stimulates c-fos transcription via phosphorylation of CREB. *Cell* 1994; 77:713-25; PMID:8205620; [http://dx.doi.org/10.1016/0092-8674\(94\)90055-8](http://dx.doi.org/10.1016/0092-8674(94)90055-8)
44. Bonni A, Brunet A, West AE, Datta SR, Takasu MA, Greenberg ME. Cell survival promoted by the Ras-MAPK signaling pathway by transcription-dependent and -independent mechanisms. *Science* 1999; 286:1358-62; PMID:10558990; <http://dx.doi.org/10.1126/science.286.5443.1358>
45. Fox KE, Colton LA, Erickson PF, Friedman JE, Cha HC, Keller P, MacDougald OA, Klemm DJ. Regulation of cyclin D1 and Wnt10b gene expression by cAMP-responsive element-binding protein during early adipogenesis involves differential promoter methylation. *J Biol Chem* 2008; 283:35096-105; PMID:18957421; <http://dx.doi.org/10.1074/jbc.M806423200>
46. Ghorpade DS, Leyland R, Kurowska-Stolarska M, Patil SA, Balaji KN. MicroRNA-155 is required for *Mycobacterium bovis* BCG-mediated apoptosis of macrophages. *Mol Cell Biol* 2012; 32:2239-53; PMID:22473996; <http://dx.doi.org/10.1128/MCB.06597-11>
47. Giebler HA, Lemasson I, Nyborg JK. p53 recruitment of CREB binding protein mediated through phosphorylated CREB: a novel pathway of tumor suppressor regulation. *Mol Cell Biol* 2000; 20:4849-58; PMID:10848610; <http://dx.doi.org/10.1128/MCB.20.13.4849-4858.2000>
48. Coco Martin JM, Balkenende A, Verschoor T, Lallemand F, Michalides R. Cyclin D1 overexpression enhances radiation-induced apoptosis and radiosensitivity in a breast tumor cell line. *Cancer Res* 1999; 59:1134-40; PMID:10070974
49. Bartek J, Lukas J. DNA repair: Cyclin D1 multitasks. *Nature* 2011; 474:171-2; PMID:21654798; <http://dx.doi.org/10.1038/474171a>
50. Jirawatnotai S, Hu Y, Michowski W, Elias JE, Becks L, Bienvenu F, Zagodzona A, Goswami T, Wang YE, Clark AB, et al. A function for cyclin D1 in DNA repair uncovered by protein interactome analyses in human cancers. *Nature* 2011; 474:230-4; PMID:21654808; <http://dx.doi.org/10.1038/nature10155>
51. Sax JK, Fei P, Murphy ME, Bernhard E, Korsmeyer SJ, El-Deiry WS. BID regulation by p53 contributes to chemosensitivity. *Nat Cell Biol* 2002; 4:842-9; PMID:12402042; <http://dx.doi.org/10.1038/ncb866>
52. Mizushima N, Yoshimori T, Levine B. Methods in mammalian autophagy research. *Cell* 2010; 140:313-26; PMID:20144757; <http://dx.doi.org/10.1016/j.cell.2010.01.028>
53. Klionsky DJ, Abdalla FC, Abieliovich H, Abraham RT, Acevedo-Arozena A, Adeli K, Agholme L, Agnello M, Agostinis P, Aguirre-Ghiso JA, et al. Guidelines for the use and interpretation of assays for monitoring autophagy. *Autophagy* 2012; 8:445-544; PMID:22966490; <http://dx.doi.org/10.4161/auto.19496>
54. Yamamoto A, Tagawa Y, Yoshimori T, Moriyama Y, Masaki R, Tashiro Y. Bafilomycin A1 prevents maturation of autophagic vacuoles by inhibiting fusion between autophagosomes and lysosomes in rat hepatoma cell line, H-4-II-E cells. *Cell Struct Funct* 1998; 23:33-42; PMID:9639028; <http://dx.doi.org/10.1247/csf.23.33>
55. Yu L, McPhee CK, Zheng L, Mardones GA, Rong Y, Peng J, Mi N, Zhao Y, Liu Z, Wan F, et al. Termination of autophagy and reformation of lysosomes regulated by mTOR. *Nature* 2010; 465:942-6; PMID:20526321; <http://dx.doi.org/10.1038/nature09076>
56. Inoki K, Zhu T, Guan KL. TSC2 mediates cellular energy response to control cell growth and survival. *Cell* 2003; 115:57-90; PMID:14651849; [http://dx.doi.org/10.1016/S0092-8674\(03\)00929-2](http://dx.doi.org/10.1016/S0092-8674(03)00929-2)
57. Costes S, Vandewalle B, Tourrel-Cuzin C, Broca C, Linck N, Bertrand G, Kerr-Conte J, Portha B, Pattou F, Bockaert J, et al. Degradation of cAMP-responsive element-binding protein by the ubiquitin-proteasome pathway contributes to glucotoxicity in beta-cells and human pancreatic islets. *Diabetes* 2009; 58:1105-15; PMID:19223597; <http://dx.doi.org/10.2337/db08-0926>
58. Taylor CT, Furuta GT, Synnestvedt K, Colgan SP. Phosphorylation-dependent targeting of cAMP response element binding protein to the ubiquitin/proteasome pathway in hypoxia. *Proc Natl Acad Sci U S A* 2000; 97:12091-6; PMID:11035795; <http://dx.doi.org/10.1073/pnas.220211797>
59. Wong E, Cuervo AM. Integration of clearance mechanisms: the proteasome and autophagy. *Cold Spring Harb Perspect Biol* 2010; 2:a006734; PMID:21068151; <http://dx.doi.org/10.1101/cshperspect.a006734>
60. Ciechanover A. Proteolysis: from the lysosome to ubiquitin and the proteasome. *Nat Rev Mol Cell Biol* 2005; 6:79-87; PMID:15688069; <http://dx.doi.org/10.1038/nrm1552>
61. Parkhira A, Myachina F, Morrison TA, Hindi KM, Auricchio N, Karbowiczek M, Wu JJ, Finkel T, Kwiatkowski DJ, Yu JJ, et al. Tumorigenesis in tuberous sclerosis complex is autophagy and p62/sequestosome 1 (SQSTM1)-dependent. *Proc Natl Acad Sci U S A* 2011; 108:12455-60; PMID:21746920; <http://dx.doi.org/10.1073/pnas.1104361108>
62. Mathew R, Karantza-Wadsworth V, White E. Role of autophagy in cancer. *Nat Rev Cancer* 2007; 7:961-7; PMID:17972889; <http://dx.doi.org/10.1038/nrc2254>
63. Grewe M, Gansauge F, Schmid RM, Adler G, Seufferlein T. Regulation of cell growth and cyclin D1 expression by the constitutively active FRAP-p70s6K pathway in human pancreatic cancer cells. *Cancer Res* 1999; 59:3581-7; PMID:10446965
64. Nelsen CJ, Rickheim DG, Tucker MM, Hansen LK, Albrecht JH. Evidence that cyclin D1 mediates both growth and proliferation downstream of TOR in hepatocytes. *J Biol Chem* 2003; 278:3656-63; PMID:12446670; <http://dx.doi.org/10.1074/jbc.M209374200>
65. Gera JF, Mellinghoff IK, Shi Y, Rettig MB, Tran C, Hsu JH, Sawyers CL, Lichtenstein AK. AKT activity determines sensitivity to mammalian target of rapamycin (mTOR) inhibitors by regulating cyclin D1 and c-myc expression. *J Biol Chem* 2004; 279:2737-46; PMID:14576155; <http://dx.doi.org/10.1074/jbc.M309999200>
66. Li Z, Jiao X, Wang C, Shirley LA, Elsaleh H, Dahl O, Wang M, Soutoglou E, Knudsen ES, Pestell RG. Alternative cyclin D1 splice forms differentially regulate the DNA damage response. *Cancer Res* 2010; 70:8802-11; PMID:20940395; <http://dx.doi.org/10.1158/0008-5472.CAN-10-0312>
67. Zhang H, Bajraszewski N, Wu E, Wang H, Moseman AP, Dabora SL, Griffin JD, Kwiatkowski DJ. PDGFRs are critical for PI3K/Akt activation and negatively regulated by mTOR. *J Clin Invest* 2007; 117:730-8; PMID:17290308; <http://dx.doi.org/10.1172/JCI28984>
68. El-Hashemite N, Zhang H, Walker V, Hoffmeister KM, Kwiatkowski DJ. Perturbed IFN- γ -Jak-signal transducers and activators of transcription signaling in tuberous sclerosis mouse models: synergistic effects of rapamycin-IFN- γ treatment. *Cancer Res* 2004; 64:3436-43; PMID:15150095; <http://dx.doi.org/10.1158/0008-5472.CAN-03-3609>
69. Zhang H, Cicchetti G, Onde H, Koon HB, Asrican K, Bajraszewski N, Vazquez F, Carpenter CL, Kwiatkowski DJ. Loss of Tsc1/Tsc2 activates mTOR and disrupts PI3K-Akt signaling through downregulation of PDGFR. *J Clin Invest* 2003; 112:1223-33; PMID:14561707
70. Peng H, Liu J, Sun Q, Chen R, Wang Y, Duan J, Li C, Li B, Jing Y, Chen X, et al. mTORC1 enhancement of STIM1-mediated store-operated Ca(2+) entry constrains tuberous sclerosis complex-related tumor development. *Oncogene* 2013; 32:4702-11; PMID:23108404; <http://dx.doi.org/10.1038/onc.2012.481>
71. Cox LJ, Hengst U, Gurskaya NG, Lukyanov KA, Jaffrey SR. Intra-axonal translation and retrograde trafficking of CREB promotes neuronal survival. *Nat Cell Biol* 2008; 10:149-59; PMID:18193038; <http://dx.doi.org/10.1038/ncb1677>
72. Zha X, Hu Z, He S, Wang F, Shen H, Zhang H. TSC1/TSC2 inactivation inhibits AKT through mTORC1-dependent up-regulation of STAT3-PTEN cascade. *Cancer Lett* 2011; 313:211-7; PMID:22055460; <http://dx.doi.org/10.1016/j.canlet.2011.09.006>
73. Horie Y, Suzuki A, Kataoka E, Sasaki T, Hamada K, Sasaki J, Mizuno K, Hasegawa G, Kishimoto H, Iizuka M, et al. Hepatocyte-specific Pten deficiency results in steatohepatitis and hepatocellular carcinomas. *J Clin Invest* 2004; 113:1774-83; PMID:15199412